

FITNESS FOR SERVICE ASSESSMENT OF LIQUID  
STORAGE TANKS

FORHAD AHMAD





**FITNESS FOR SERVICE ASSESSMENT OF  
LIQUID STORAGE TANKS**

BY

FORHAD AHMAD

A THESIS

SUBMITTED TO THE SCHOOL OF GRADUATE STUDIES  
IN PARTIAL FULFILLMENT OF THE  
REQUIREMENTS FOR THE DEGREE OF  
MASTER OF ENGINEERING

FACULTY OF ENGINEERING AND APPLIED SCIENCE  
MEMORIAL UNIVERSITY

St. John's, NL, Canada

October 2009

## ABSTRACT

Storage tanks are widely used in industrial applications in order to store liquid products. Corrosion damage, which is generally termed as locally thinned area (LTA), is considered to be a serious threat to the structural integrity of the industrial storage tanks. Therefore, fitness-for-service (FFS) assessment of these structures needs to be performed periodically in order to ensure the operational safety and structural integrity.

In the present work, the Remaining Strength Factor (RSF) is chosen to quantify corrosion damage. Two alternative methods are proposed for FFS assessment of industrial storage tanks undergoing corrosion damage. The methods are based on the variational concepts in plasticity, the  $m$ -alpha tangent multiplier, the concept of elastic decay lengths and the idea of reference volume. The proposed methods are shown to give conservative assessment of the remaining strength of storage tanks developing LTA during operation. The methods are demonstrated through an example, and the results are verified by inelastic finite element analysis.

## **Acknowledgements**

I would like to thank Dr. R Seshadri for his invaluable guidance and patience during the different phases of the thesis development. His vast knowledge and immense expertise in diversified areas provided me with working on an industrial project. I am also grateful for the financial support provided by Dr. R Seshadri and the Faculty of Engineering and Applied Science during the course of my graduate studies.

I would also like to thank Dr. S. M. R. Adluri for his help and support. I would like to extend my acknowledgement to my colleagues in the Asset Integrity Management Research Group for their kind assistance and support. I would also like to thank Mrs. Heather O' Brien for her support in the documentation and printing activities. I also thank the Associate Dean of Graduate Studies, and acknowledge Mrs. Moya Crocker, Office of the Associate Dean, for her administrative assistance during the course work. I owe my deepest thanks to my family: my father, my mother, my sister and brother for their inspiration and encouragement.

# CONTENTS

## CHAPTER 1

### INTRODUCTION

1.1 Background .....	1
1.2 Structural Integrity Assessment .....	3
1.3 Objective of the Research .....	5
1.4 Structure of the Thesis .....	6

## CHAPTER 2

### LIQUID STORAGE TANKS

2.1 Introduction to Storage Tanks .....	8
2.2 Tank Selection Criteria .....	10
2.3 Classification of Above Ground Storage Tanks .....	12
2.4 Tank Base Design .....	14
2.4.1 Foundation .....	14
2.4.2 Tank Bottom.. .....	16
2.5 Tank Roofs .....	17

2.6	Materials of Construction .....	18
2.7	Corrosion of Tanks .....	19
2.8	Corrosion Detection in Storage Tanks .....	20
2.9	Closure .....	27

## CHAPTER 3

### BASIC CONCEPTS IN PLASTICITY

3.1	Introduction .....	28
3.2	Theory of Plasticity .....	29
3.2.1	The Yield Criteria .....	29
3.2.2	Yield Surface .....	33
3.3	Theoretical Consideration .....	34
3.3.1	Classical Lower Bound Multiplier .....	35
3.3.2	Upper Bound Multiplier .....	36
3.3.3	The $m_a$ Multiplier.....	38
3.3.4	The $m_a$ -Tangent .....	40
3.3.5	Blunting of Peak Stresses.....	43
3.3.6	Significance of $\zeta^*=1+\sqrt{2}$ .....	44
3.3.7	The $m_a$ -Tangent Method.....	45
3.4	Remaining Strength Factor (RSF) .....	48

3.4.1	RSF Based on the Upper Bound Multiplier .....	50
3.4.2	RSF Based on the $m_u$ -Tangent Multiplier .....	51
3.4.3	RSF Based on Classical Lower Bound Multiplier .....	52
3.5	Inelastic Finite Element Analysis .....	53
3.6	Hydrostatic Pressure in Liquid Storage Tanks.....	55
3.7	Closure .....	59

## CHAPTER 4

### FITNESS FOR SERVICE (FFS) PROCEDURE

4.1	Introduction.....	60
4.2	Effective Area Methods.....	61
4.2.1	ASME B31G.....	63
4.2.2	Modified ASME B31G criterion.....	64
4.2.3	RSTRENG.....	65
4.3	Fitness-For-Service Assessment Procedure .....	67
4.4	API 579 Evaluation Procedure .....	69
4.4.1	Level 1 Assessment procedure from API 579.....	70
4.4.2	Level 2 Assessment procedure from API 579.....	72
4.5	Factors Influencing Corrosion Failure .....	73
4.6	Methodology for Proposed Level 2 Fitness-For-Service (FFS)Evaluation for Liquid	

Storage Tanks .....	76
4.7 Decay Length and Reference Volume .....	78
4.8 Closure .....	81

## CHAPTER 5

### APPLICATION TO CYLINDRICAL STORAGE TANK

5.1 Introduction .....	82
5.2 Finite Element Modeling .....	84
5.3 Material Model.....	86
5.4 Illustrative Example .....	88
5.4.1 Required Thickness calculation .....	90
5.4.2 Calculation of Decay Lengths .....	90
5.4.3 Evaluation of Hydrostatic Equivalent Pressure .....	91
5.4.4 Evaluation of Multipliers .....	94
5.5 RSF Using Analytical Approach .....	95
5.6 RSF Using Two Linear Elastic FEA .....	96
5.7 RSF Based on Inelastic FEA .....	97
5.8 Discussion.....	100

## CHAPTER 6

### CONCLUSIONS, RECOMMENDATIONS AND FUTURE WORKS

6.1 Contributions of this Thesis .....	102
6.2 Future Effort .....	103
6.3 Conclusions.....	105
▪ <b>Publications</b> .....	106
▪ <b>References</b> .....	107
▪ <b>Appendix A ANSYS Input Files</b> .....	114
A.1 Linear Analysis of Storage Tank without Corrosion Subjected to Internal Pressure	
A.2 Non-linear Analysis of Storage Tank without Corrosion Subjected to Internal Pressure	
A.3 Linear Analysis of Storage Tank with Corrosion Depth 25% Subjected to Internal Pressure	
A.4 Non-linear Analysis of Storage Tank with Corrosion Depth 25% Subjected to Internal Pressure	

## LIST OF TABLES

<b>Table 4.1</b>	Factors influencing the Behavior of LTA.....	74
<b>Table 5.1</b>	RSF for Liquid Storage Tank having LTA with 25% corrosion.....	98
<b>Table 5.2</b>	RSF for Liquid Storage Tank having LTA with 50% corrosion.....	99

## LIST OF FIGURES

<b>Figure 2.1</b>	Typical Large Diameter Storage Tank.....	9
<b>Figure 2.2</b>	Tank Selection Criterion .....	11
<b>Figure 2.3</b>	Type of Roofs.....	17
<b>Figure 3.1</b>	Von Mises and Tresca Yield Criteria .....	32
<b>Figure 3.2</b>	Yield Surfaces .....	34
<b>Figure 3.3</b>	Regions of lower and upper bounds of $m_a$ .....	39
<b>Figure 3.4</b>	The $m_a$ -tangent construction.....	42
<b>Figure 3.5</b>	Stress distribution ahead of notch tip. ....	43
<b>Figure 3.6</b>	A schematic diagram of rectangular LTA in a storage tank.....	56
<b>Figure 3.7</b>	Graphical representations of hydrostatic forces on a vertical rectangular surface .....	57
<b>Figure 4.1</b>	Procedure to establish the critical thickness profiles.....	66

<b>Figure 4.2</b>	Subdivision process for Determining the RSF .....	72
<b>Figure 4.3</b>	Schematic diagram of primary factors controlling the behavior of locally thinned areas .....	75
<b>Figure 4.4</b>	Rectangular Equivalent Area in Cylindrical Vessel.....	76
<b>Figure 4.5</b>	Contributing parameters to the proposed Level 2 evaluation methods.....	77
<b>Figure 4.6</b>	Decay length and reference volume dimensions for cylindrical shell.....	80
<b>Figure 5.1</b>	Material Model for Finite Element Analysis.....	87
<b>Figure 5.2</b>	A schematic diagram of rectangular LTA in a storage tank.....	89
<b>Figure 5.3</b>	Evaluation of Hydrostatic Equivalent Pressure .....	92

## Abbreviations

LEFEA	Linear Elastic Finite Element Analysis
LTA	Locally Thinned Area
NFEA	Nonlinear Finite Element Analysis
RSF	Remaining Strength Factor
AST	Above Ground Storage Tank
UST	Under Ground Storage Tank
FCA	Future Corrosion Allowance
FEA	Finite Element Analysis
FFS	Fitness-for-Service

## Nomenclature

$a$	half of the LTA in circumferential direction
$b$	half of the LTA in longitudinal direction
$E$	modulus of elasticity
$h$	uncorroded shell thickness
$h_c$	corroded shell thickness
$m$	exact limit load multiplier
$m_L$	classical lower bound limit load multiplier
$m^0$	upper bound limit load multiplier
$m_\alpha$	m-alpha multiplier
$P$	applied load
$V_T$	total volume
$X_C$	decay length in circumferential direction
$X_L$	decay length in longitudinal direction
$\zeta$	ratio of $m^0/m_L$
$\sigma_{eq}$	von Mises equivalent stress
$\sigma_y$	yield stress

### Subscript

$eq$	von Mises equivalent
$L$	limit
$y$	yield

Superscript

0            statically admissible quantities

$T$             tangent

# CHAPTER 1

## INTRODUCTION

### 1.1 BACKGROUND

Storage tanks are an important component in the technological chain of the processes involving extraction, storage, transportation and the processing of crude oil and gas. According to the survey conducted by American Petroleum Institute (API), there are about 700,000 petroleum storage tanks in North America.

Industrial storage tanks are generally used to store liquid petroleum products. From the instant a storage tank is commissioned it begins to deteriorate. Although storage tanks are of importance in the petroleum industry failures due to corrosion defects have become a significant, recurring and an expensive operational, safety and environmental concern. Storage tanks experiences external corrosion due to environmental conditions on the exterior surface of the steel tank (e.g. from the natural chemical interaction between the exterior of the tank and the air, water or soil surrounding it). Internal corrosion occurs in steel storage tank due to chemical attack on the interior surface of the tank due to the commodity stored. Liquid storage tanks generally experience differential hydrostatic

pressure due to the stored liquid head, while the pressure vessels and piping systems generally experience uniform pressure. Therefore, the structural behavior of the storage tanks is different than that of structures like pressure vessels and piping.

When local metal loss occurs in industrial storage tanks due to corrosion, the Locally Thin Area (LTA) undergoes higher deformation than the surrounding undamaged region. This differential deformation of the structure is generally termed as “bulging”. Excessive bulging in a pressurized component is undesirable and is a considerable threat to the structural integrity. In practice, the so-called “Folias factor” is used to quantify the bulging effect at LTAs in shell structures. The phenomenon exists in the case of internal pressure and is more pronounced in shells with smaller diameter e.g., piping. Industrial storage tanks generally have a very large diameter and hence the use of this parameter is not relevant.

On account of the hydrostatic head in the storage tank, the LTA or the corroded region bulges outward. This bulging effect produces bending moments at the edge of the LTA with the surrounding shell. The magnitude and significance of the bending moments depends on the size and relative thickness of the LTA compared to the surrounding wall thickness. If the thickness of the LTA is very large compared to the surrounding wall thickness, then the effect of the edge bending moment becomes significant.

## 1.2 STRUCTURAL INTEGRITY ASSESSMENT

Structural integrity assessment is one of the principal tasks that has been implemented by the petrochemical, nuclear power generation and oil and gas industries. It plays a major role in preserving safety and economy of the plant, equipment and system operation. Integrity assessment is a multidisciplinary effort and with regard to the oil and gas industries; it involves interactions of diverse fields such as process chemistry, process engineering, thermo-fluids, mechanics, materials, applied physics and computational technology. The assessment activities are carried out in three phases: design, construction and post construction. The post construction activity is subdivided into operations, inspection, maintenance and restoration activities.

Structural integrity assessment in the oil and gas industry is practiced in three levels. Level 1 assessment procedures provide conservative screening criteria that can be used with a minimum quantity of inspection data or information about the component. Level 2 is intended for use by facilities or field engineers, although some owner-operator organizations consider it suitable for a central engineering evaluation. Level 3 assessments require sophisticated analysis by experts, where advanced computational procedures are often carried out.

Recommended practices and procedures associated with FFS assessment are available in API 579 [1], R6 [2], SINTAP [3], and RSTRENG [4]. The practice for conducting FFS assessments for pressurized components in oil and gas sector is API 579 [1], in which the procedures are based on ASME B31G and the RSTRENG criteria. The API 579 assessment provides a consistent result for regions of metal loss with significant thickness variability. Sims et al. [12] have studied LTA in gas storage tanks in the context of FFS assessment. They have reported results of some parametric analysis using inelastic FEA, and have attempted to provide empirical equations for FFS assessment. Development of a comprehensive assessment criterion for the corroded liquid storage tank is difficult due to the numerous variables (tank geometry, defect geometry, material properties and hydrostatic pressure) influencing the behavior and failure of the corroded region.

### **1.3 OBJECTIVE OF THE RESEARCH**

The current study will focus on developing an improved Level 2 FFS assessment method for the structural integrity assessment of industrial storage tanks undergoing corrosion damage. The study of the fitness-for-service assessment methodology assumes elastic-plastic ductile material which is able to absorb significant deformation beyond the elastic limit without the danger of fracture. Strain hardening is assumed to be small for the entire analysis.

Internal differential hydrostatic pressure due to stored liquid head is assumed to be the only significant load in this work. Corrosion damage will be considered for a tank with the remaining thickness ratio (defined as the ratio of the corroded wall thickness to the nominal thickness) not less than 0.5. The storage tank studied in the current work is assumed to be originally designed and constructed in accordance with a recognized code or standard. Therefore two alternative methods are proposed. The first approach is based on an analytical method, and the second approach is based on two linear elastic finite element analysis (LEFEA). The proposed methods are shown to give a conservative assessment of the remaining strength of storage tanks containing local thin areas (LTAs). The results obtained from the proposed Level 2 assessment procedure are found to be in good agreement with the corresponding inelastic finite element results.

## 1.4 STRUCTURE OF THE THESIS

This thesis is composed of six chapters. The first chapter of the thesis addresses the general background, objectives and scope of the proposed research work.

Chapter 2 presents a brief review of literature. This chapter covers theoretical aspects of liquid storage tanks, tank selection criteria and types of storage tanks. This chapter also covers a review of tank base design, materials, corrosion and corrosion detection in storage tanks according to recognized code and standards.

Chapter 3 presents a brief review of literature pertaining to the current research work. The chapter covers theoretical aspects of plasticity, the classical lower and upper bound limit load multipliers and the  $m_n$ -tangent multiplier method which is the basis of the current research. This chapter also describes the evaluation of hydrostatic pressure on the storage tank containing corrosion damage.

Chapter 4 studies the factors influencing the behavior of pressure vessels containing corrosion damage. The general methodology of the proposed Level 2 Fitness-for-Service assessment based on the concept of reference volume is also presented.

In chapter 5, finite element modeling details for the present study and materials model is discussed. Illustrative numerical examples are provided. The recommended methods for

proposed Level 2 Fitness-for-Service assessments are validated by Level 3 inelastic finite element analysis.

Chapter 6 summarizes the original contributions to this thesis. This chapter also concludes by providing recommendations on future research work in this area.

## **CHAPTER 2**

### **LIQUID STORAGE TANKS**

#### **2.1 INTRODUCTION TO STORAGE TANKS**

The word Storage Tank identifies only a single type or piece of equipment in an industrial facility. Tanks have been used in innumerable ways both to store every conceivable liquid, vapor and in a number of processing applications. For this present work a tank primarily is considered as a vertical liquid storage vessel.

The analysis and design of welded steel tanks for hydrocarbon storage are based on the API Standard 650 [18]. The standard is applicable to storage tanks of various sizes and capacities operating at internal pressures close to atmospheric pressure.

Storage tanks used for storing hydrocarbon are usually large in diameter. Large diameter liquid Storage tanks have different course thickness and are built on either a compacted fill or concrete ring wall foundation. Large diameter storage tanks are usually field erected due to economic considerations and ease of construction. A typical large diameter field erected storage tank having a height of 576 inches and a radius of 1728 inches and a capacity of 500,000 barrels is shown in Figure 2.1 [36].

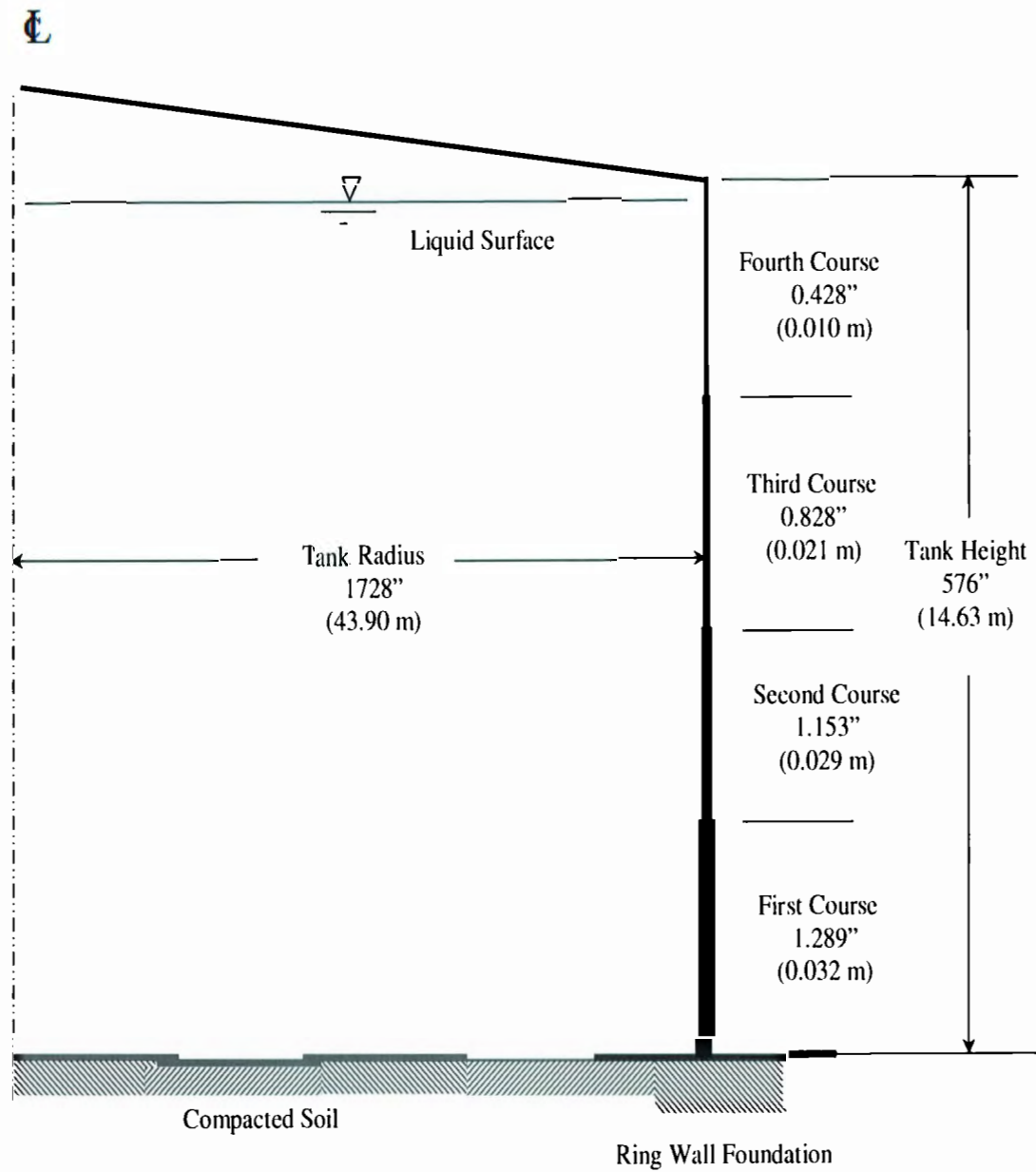


Figure 2.1. Typical Large Diameter Storage Tanks [36]

## 2.2 TANK SELECTION CRITERIA

The selection of tanks is a complex process of optimizing an array of information to yield a particular design as, indicated in Fig.2.2. Several factors must be considered when selecting the various characteristics of a proposed storage tank system. The characteristics include:

- AST or UST;
- Tank Material;
- Single or Double Wall Tank;
- Piping materials.

As shown in the Fig.2.2, once the specific liquid to be stored is established, the physical properties then determine the range of possible tank types. Although vapor pressure is a major component in tank selection, other properties such as flash point, potential for explosion, temperature and specific gravity all factor in the selection and design of tanks.

In addition to fundamental physical properties influencing tank selection, size, regulations, current best practices and external loads (such as wind, snow and seismic loads), as well as numerous additional engineering issues, play a role. The ultimate selection criteria are keenly dependent on the actual site-specific conditions, local regulations, cost considerations, required operating life, potential for fires and explosion and many other factors.

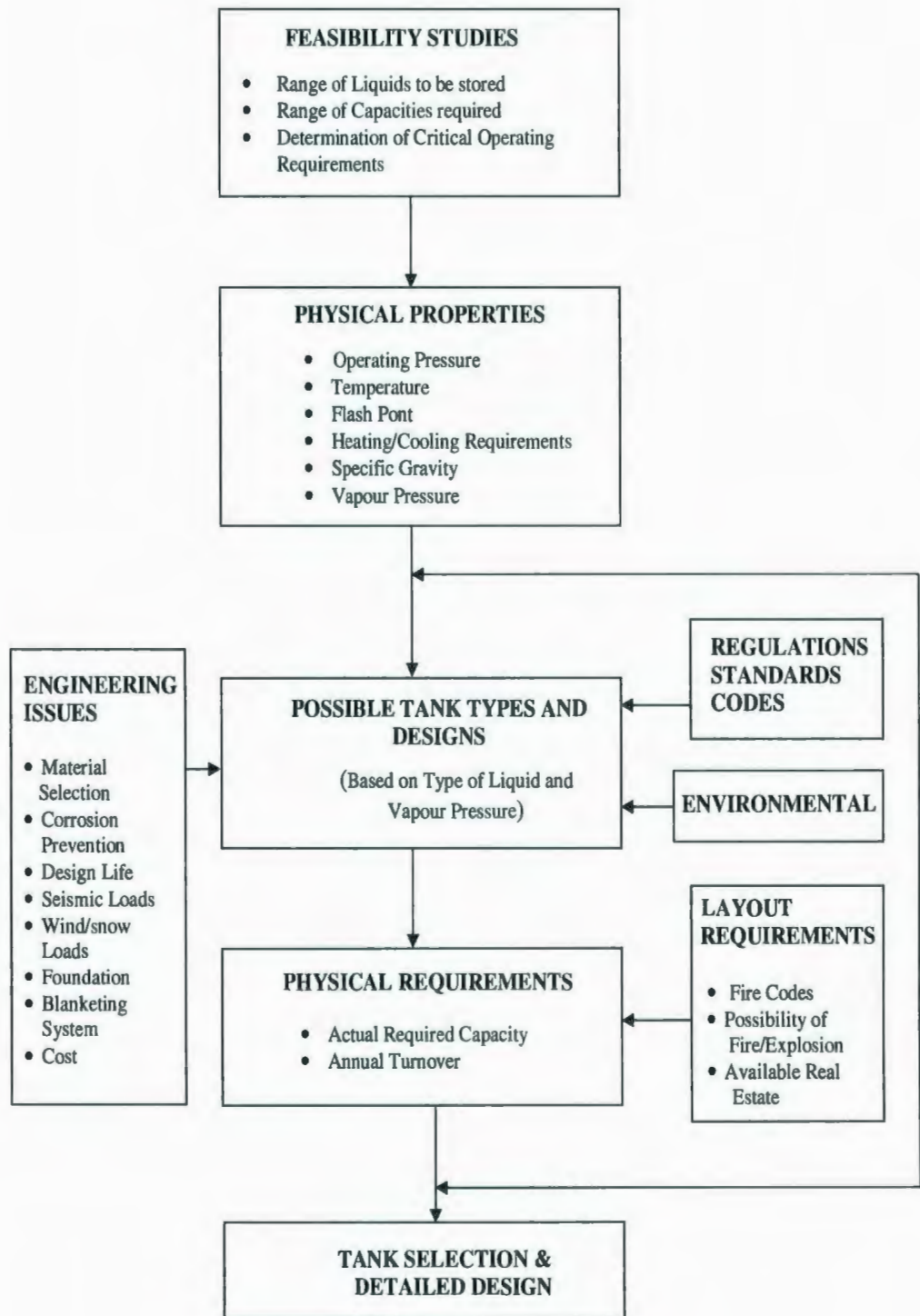


Figure 2.2 Tank Selection Criteria [31]

## **2.3 CLASSIFICATION OF ABOVE GROUND STORAGE TANKS**

There are many ways to classify a tank, but there is no universal method. However, a classification commonly employed by codes, standards and regulations is based on the internal pressure of a tank. This method is useful in that it depends on a fundamental physical property to which all tanks are subjected internal or external pressure. In this present work only Above Ground Storage Tanks (AST) that are used extensively are considered.

### **2.3.1 Atmospheric Tanks**

The most common type of tank is the atmospheric tank. Although called atmospheric, these tanks are usually operated at internal pressure slightly above atmospheric pressure around ½ psi (3.447 kpa). The fire codes define an atmospheric tank as operating from atmospheric up to ½ psi (3.447 kpa) above atmospheric pressure. The API 650 [18] governs the design, material, fabrication, erection and testing requirements for above ground vertical cylindrical storage tanks of various sizes and capacities for internal pressures approximating atmospheric pressures.

### **2.3.2 Low Pressure Tanks**

Low pressure in the context of tanks means tanks designed for a higher pressure than atmospheric tanks. These tanks are designed to operate from atmospheric pressure up to 15 psi.

### **2.3.2 High Pressure Tanks (Pressure Vessels)**

Since high pressure tanks (vessels operating above 15 psi) are actually pressure vessels, the term high-pressure tank are not used by those working with tanks. Because pressure vessels are a specialized form of container and are treated separately from tanks by all codes, standards and regulations. The ASME Boiler and Pressure Vessel Code [48] is one of the primary standards that have been used throughout the world to ensure safe storage vessels.

Various substances such as ammonia and hydrocarbons are frequently stored in spherically shaped vessels which are often referred to as tanks. Most often the design pressure is above 15 psi and they are really spherical pressure vessels and their design and construction fall under the rules of the ASME Boiler and Pressure Vessel Code.

## **2.4 TANK BASE DESIGN**

The design of the storage tank base depends upon several factors:

- The type of foundation (earth grade, compacted or concrete ring wall).
- Size of the storage tank.
- The operating temperature of the tank.
- Corrosiveness of the liquid.
- Amount of sedimentation of suspended solids.

### **2.4.1 Foundations**

The type of construction and the configuration of the foundation are very relevant factors from a standpoint of design and operation of the tank. While it is difficult to classify all possible foundation types for storage tanks, some general types have proved to be most common for specific applications. Foundation types may be broken into several classifications in generally increasing order of costs:

- Compacted soil.
- Crushed-stone ring wall.
- Concrete ring wall.
- Slab.
- Pile-supported.

Depending on the type of foundation, appropriate tolerances must be maintained. If a concrete ring wall is provided under the shell-to-annular plate connection, the top of the ring wall must be level within  $\pm 1/8$  inch, in any 30 feet circumference, and  $\pm 1/4$  inch, in a total circumference measured from the average elevation [18]. If a concrete ring wall not utilized i.e. compacted foundation, the specified tolerance of the shell level should be within  $\pm 1/8$  inch, over any 10 feet circumference with  $\pm 1/2$  inch, in total circumference measured from the average elevation.

Tolerances are specified for the tank foundation, because they have a direct effect on the behavior of the tank shell and any components connecting to the shell. If the tolerances are exceeded tank behavior will be affected. In this current work mainly the shell is taken in consideration to evaluate the Remaining Strength Factor (RSF) of a storage tank.

## 2.4.2 Tank Bottom

The shapes of cylindrical storage tank closures (e.g., top and bottom) are a strong function of the internal pressure. Because of the varying condition to which a tank bottom may be subjected, several types of tank bottoms have evolved. Tank bottom classifications may be broadly classified by shapes as:

- Flat-bottom.
- Conical.
- Domed or spheroid.

Because flat-bottom tanks usually have a small designed slope and shape, they are sub classified according to the following categories:

- Flat
- Cone up
- Cone down
- Single -slope

Tank bottom design is important because sediment, water, or heavy phases settle at the bottom. Corrosion is usually the most severe at the bottom, and the design of the bottom can have a significant effect on the life of the tank.

## 2.5 TANK ROOFS

The type of roof used on liquid storage tanks presents an important design consideration. Liquid storage tanks at refineries are generally fixed roof tanks, external floating roof tanks and internal floating roof tanks. If vapor pressure is less than 1.5 psi, open top tanks or fixed-roof tanks works well. Fixed-roof tanks greatly reduce the risk of fire and limit the amount of vapor that evaporates, when compared with open top tanks. Floating roof is used to reduce the probability of combustible gas mixture for certain volatile petroleum products having a vapor pressure higher than 1.5 psi. Roofs of low pressure atmospheric storage tanks can be divided into the following way:

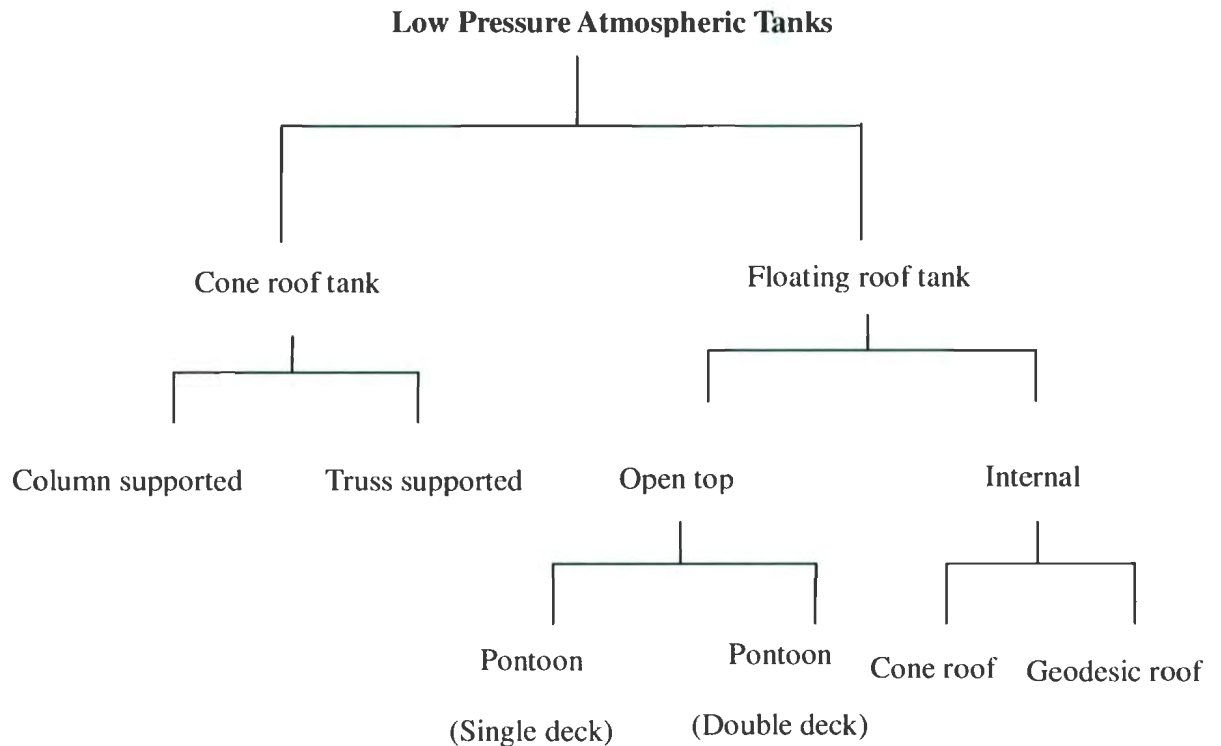


Figure 2.3 Types of Roofs [30]

## 2.6 MATERIALS OF CONSTRUCTION

Materials selection for above ground vertical cylindrical storage tanks of various sizes and capacities for internal pressures approximating atmospheric pressure is based upon the API Standard 650. But the principles are applicable to other codes such as API 620 [19] or AWWA D-10 [30]. Materials for tanks are selected on the basis of four primary characteristics:

- Corrosion resistance: resistance to wall thinning, pitting, cracking and metallurgical transformation.
- Shop and field fabricability: ease of transport, assembly, and erection, including bending, machining, welding and coating.
- Mechanical properties: strength, ductility, and toughness, through the operating temperature range (from creep temperatures down to cryogenic service).
- Cost.

The construction of new tanks in the different temperature categories is covered by API Standards 650 [18] and 620 [20]. API Standard 650 covers the construction of storage tanks for ambient temperature operation. Appendix M of API 650 covers tank design temperatures between 200<sup>0</sup>F and 500<sup>0</sup>F by applying a derating factor for the allowable stresses of the steels. For low-temperature tanks, API Standard 620 gives specific material requirements that allow for operation to as low as -270<sup>0</sup>F.

## 2.7 CORROSION OF TANKS

Industrial storage tanks are used to store liquid products. These tanks experience hydrostatic pressure due to the liquid head, while pressure vessels and piping systems generally experience uniform pressure. When corrosion occurs in storage tanks, the LTA undergoes higher deformation than the surrounding undamaged region. Excessive bulging in a pressurized component is undesirable and can be a threat to the structural integrity.

Most tanks are made of carbon steel, which can corrode when exposed to air and water. Over time, uncontrolled rusting can weaken or destroy the components of a tank, resulting in holes or possible structural failure, and release of stored products into the environment.

Rusting in storage tank can be accelerated by factors including:

- Increased temperature.
- Corrosive environment.
- Stray electric currents between interconnected components.

## 2.8 CORROSION DETECTION IN STORAGE TANKS

To evaluate the Remaining Strength Factor (RSF) of an in-service component metal loss should be detected properly. Several non destructive inspection techniques are available to inspect tanks; vessels and piping are presented by API 579. The choice of the technique depends on the material, the type of flaw, access to the surface, availability, and cost.

Typical monitoring methods include the use of the following tools or procedures:

- UT measurements and scanning
- Radiographic examination
- Magnetic particle testing
- Thermography
- Liquid Penetration Testing
- Eddy Current Testing
- Corrosion probes
- Hydrogen probes
- Laser profiling
- Visual Examination

The keys to accurate inspections are:

- Inspection technique consistent with expected damage.
- Expertise and qualifications of inspectors
- Independence of inspector
- Cleanliness of component
- Access to the component
- Good quality, calibrated instruments

### **2.8.1 Ultrasonic Testing (UT)**

Thickness readings which are required to determine the metal loss on a component are usually made using straight beam ultrasonic thickness examination (UT). This method can provide high accuracy and can be used for point thickness readings and obtaining thickness profiles. Advantages of Ultrasonic thickness examination is, only one side needs to be accessed and can be used on complex shapes. The limitations of UT are associated with uneven surfaces and access. Obtaining accurate thickness reading using UT is highly dependent on the surface condition of the component. Surface preparation techniques vary depending on the surface condition, but in many cases wire brushing is sufficient. However, if the surface has a scale build-up or is pitted, grinding may be

necessary. Temperature compensation and special UT couplants are required if the thickness readings are obtained on high temperature components.

### **2.8.2 Radiographic Testing (RT)**

Radiographic Testing (RT) may also be used to determine metal loss; however, accurate thickness data may only be obtained by moving the component containing the metal loss, or moving the source around the component to obtain multiple views. This type of manipulation is typically not possible for many pressure containing components. However, RT examination can be effectively used to qualify the existence, extent and depth of a region of metal loss, and has been used in conjunction with UT to determine whether the metal loss on a component is general or local.

#### Advantages of RT

- Detects surface and volumetric flaws.
- Covers a relatively large area.
- Provides a permanent record (film or digital)
- Recognized by construction codes.
- Detects narrow, crack like flaws.

### Limitations of RT

- Requires a personnel exclusion zone.
- Requires experienced, certified operators.
- Requires an X-ray or gamma-ray (radioactive source).
- Gamma rays have limited life.
- It is difficult to decipher radiographies of complex shapes.
- Detects length of crack like flaws, but may not characterize their depth.

### 2.8.3 Magnetic Particle Testing (MT)

A magnetic field is created on the surface of the part, for example, by using a yoke and a powder or solution of magnetic particles is dispersed on the surface. The magnetic particles orient themselves along the magnetic lines, and surface discontinuities become visible as the magnetic lines appear distributed. Wet fluorescent magnetic particles are particularly well suited for the examination of pipe, vessels, and tank welds. The advantages of using the magnetic particle testing is flaws do not have to be open to the surface, portable, detects surface and slightly subsurface flaws. This technique is applicable only to ferromagnetic materials; surface must be sufficiently smooth to permit particle movement. This technique of inspection to be followed by vapor degreasing or chemical cleaning.

### Advantages of MT

- Detects surface and slightly subsurface flaws.
- Flaws do not have to be open to the surface.
- Portable.

### Limitations of MT

- Applies only to ferromagnetic materials.
- Surface techniques cannot determine depth of flaw.
- Discontinuities only detected if perpendicular to magnetic field.
- Surface must be sufficiently smooth to permit particle movement.
- Inspection to be followed by vapor degreasing or chemical cleaning.
- No permanent record.

#### **2.8.4 Eddy Current Testing**

Eddy currents are generated by a probe into the wall of a specimen. The presence of a flaw in the wall or a change in wall thickness will be detected by a disturbance of the current.

Pulsed eddy currents are used to measure wall thinning under insulation. Changes in the wall thickness can be detected on pipe wall thickness from 0.3 into 1.5 in, with accuracy on the order of a few mils. This ability to measure wall thickness while the line is in service and without removing insulation can lead to significant cost savings.

#### **2.8.5 Visual Examination**

Visual examination (Visual Testing, VT) is the most common examination technique. It can be direct or assisted for remote access, for example, through mirrors, borescope, and cameras. Pipe Fabrication Institute Standard ES-27 defines visual examination as examination with the “unaided eye,” other than the use of corrective lenses, within 24 in. Examiners are classified in increasing order of qualification from VT-1 to VT-3.

### 2.8.6 Liquid Penetration Testing (PT)

A visible or fluorescent penetrant is applied to the surface for a few minutes (dwell time), during which time the penetrant seeps into surface connected flaws. The excess penetrant that did not penetrate the flaws is then wiped away. Finally, a contrasting spray or powder developer is applied to draw the penetrant back to the surface by capillary action. This will outline the flaw shape.

#### Advantages of PT

- Can be used on uneven surfaces.
- Portable.

#### Limitations of PT

- Flaw must be open to the surface.
- Affected by surface cleanliness, roughness.
- No permanent record.
- Surface technique cannot determine depth of flaw.
- Inspection to be followed by vapor degreasing or chemical cleaning.

## **2.9 CLOSURE**

The current chapter provides the information about liquid storage tanks. An overview of the tank selection criteria is presented. Research work here in is limited to above ground storage tanks system, the tank base design, foundations; materials of construction are presented accordingly. Corrosion in liquid storage tanks is described briefly, and corrosion detection procedures are presented in this section according to the recognized codes and standards.

## **CHAPTER 3**

### **BASIC CONCEPTS IN PLASTICITY**

#### **3.1 INTRODUCTION**

This chapter presents a summary of the theoretical concepts pertaining to the proposed research work. A brief review of theory of plasticity, limit analysis including limit load multipliers and estimations of remaining strength factor for storage tanks is presented. Evaluation of hydrostatic pressure on liquid storage tanks and inelastic finite element analysis is also covered briefly. Literature regarding Fitness-for-Service assessments for liquid storage tanks containing corrosion damage from previous investigations is reviewed and discussed. These theories and concepts are used extensively in this current research work.

## **3.2 THEORY OF PLASTICITY**

For limit analysis of components or structures theory of plasticity is considered as the basis. Structures or components are assumed to reach a certain limiting plastic state of the material before failure.

In the plastic range, the strains are dependent on the history of loading. In order to determine the final plastic strain, the incremental strains must be added over the full loading history. The principles and mathematical interpretations of the theory of plasticity and its field of applications are available in [29].

### **3.2.1 The Yield Criteria**

When the stress is uniaxial, a yield point at which the material begins to deform plastically can be readily determined. On the other hand, when the material is subject to multiaxial stresses yielding will occur. The most common yield criteria which are generally termed as failure theories for metal structures are briefly discussed below.

### 3.2.1.1 Tresca Yield Criterion (Maximum Shear Stress Theory)

Maximum shear stress theory assumes that yielding will occur when the maximum shear stress in multi-axial state of the stress reaches the value of the maximum shear stress occurring under simple tension test. The maximum shear stress is equal to half the difference between the maximum and minimum principle stresses. For simple tension, only one principle stress exists (i.e  $\sigma_1 = \sigma_y$ ) and  $\sigma_2 = \sigma_3 = 0$ . If the principle stresses are  $\sigma_1$ ,  $\sigma_2$  and  $\sigma_3$  ( $\sigma_1 > \sigma_2 > \sigma_3$ ). According to Tresca yield Criterion, yielding will occur when,

$$\left| \sigma_1 - \sigma_3 \right| = \sigma_y \quad (3.1)$$

where  $\sigma_y$  is the yield strength of the material. The Tresca yield criterion takes the form of a hexagon in two-dimensional stress space. The size of the hexagon depends on the yield strength of the material. The plot of the Tresca yield criterion for a two-dimensional state of stress is shown in figure 3.1. The Tresca yield criterion is used extensively in design because of it simplifies the analysis and design, and is slightly conservative compared to the Von Mises criterion.

### 3.2.1.2 Von Mises Criterion (Distortion Energy Theory)

Due to the elastic deformation strain energy is stored in the material. This deformation can be viewed as a combination of volume change and angular distortion without volume change. The energy that is stored in the body due to angular distortion is called the shear strain energy or distortion energy.

The distortion energy theory assumes that yield begins when the distortion energy equals the distortion energy at yield in simple tension. The distortion energy can be calculated as  $U_d = 1/ (2G) J_2$  , where  $G$  is the shear modulus and  $J_2$  is the second invariant of the deviatoric stress tensor which can be written in terms of principle stresses as :

$$J_2 = 1/6 [(\sigma_1 - \sigma_2)^2 + (\sigma_1 - \sigma_3)^2 + (\sigma_3 - \sigma_2)^2] \quad (3.2)$$

At the yield point in simple tension,  $J_2 = 1/3 \sigma_y^2$ . The von Mises yield criterion can be expressed as

$$[(\sigma_1 - \sigma_2)^2 + (\sigma_1 - \sigma_3)^2 + (\sigma_3 - \sigma_2)^2] = \sigma_y^2 \quad (3.3)$$

The plot of the von Mises yield criterion for a two dimensional state of stress is shown in the figure 3.1

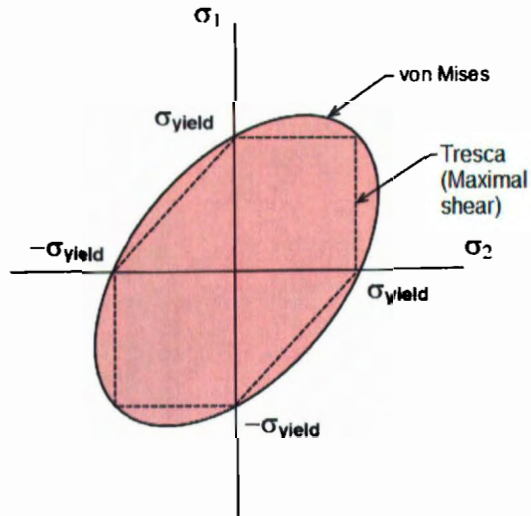


Figure 3.1: Von Mises and Tresca Yield Criteria [17]

In the Figure 3.1 it is observed that Tresca's yield surface is circumscribed by von Mises. Therefore, it predicts plastic yielding already for stress states that are still elastic according to the von Mises criterion. As a model for plastic material behavior, Tresca's criterion is therefore more conservative compared to the von Mises yield criterion as it relates to failure.

### 3.2.2 Yield Surface

Generally, the yield criterion depends on the complete three-dimensional state of stress at the point under consideration. For a material loaded to the initial yield, the relationship for a yield criterion can be expressed as,

$$f(\sigma_{ij}) = K \quad (3.4)$$

where,  $\sigma_{ij}$  is a stress tensor in three dimensional space,  $K$  is a known function. Equation (3.4) is called *yield function* and represents a hyper surface called *yield surface*. Any point on this surface essentially indicates the beginning of yielding. The yield surface is usually expressed in terms of (and visualized in) a three-dimensional principal stress space ( $\sigma_1, \sigma_2, \sigma_3$ ), a two- or three-dimensional space spanned by stress invariants ( $J_1, J_2, J_3$ ) or a version of the three-dimensional Haigh–Westergaard space. In the Haigh–Westergaard stress space for principle stress ( $\sigma_1, \sigma_2, \sigma_3$ ) coordinate system, a line having equal angles with the coordinate axes (i.e.,  $\sigma_1 = \sigma_2 = \sigma_3 = \sigma_m$ ) corresponds to a hydrostatic stress state where the deviatoric stresses are equal to zero. The yield surface is plotted as a cylinder or prism along this line for Von Mises or Tresca criterion, respectively. The intersection of this yield surface with any plane perpendicular to the centerline will produce a curve called the yield locus (Figure 3.2)

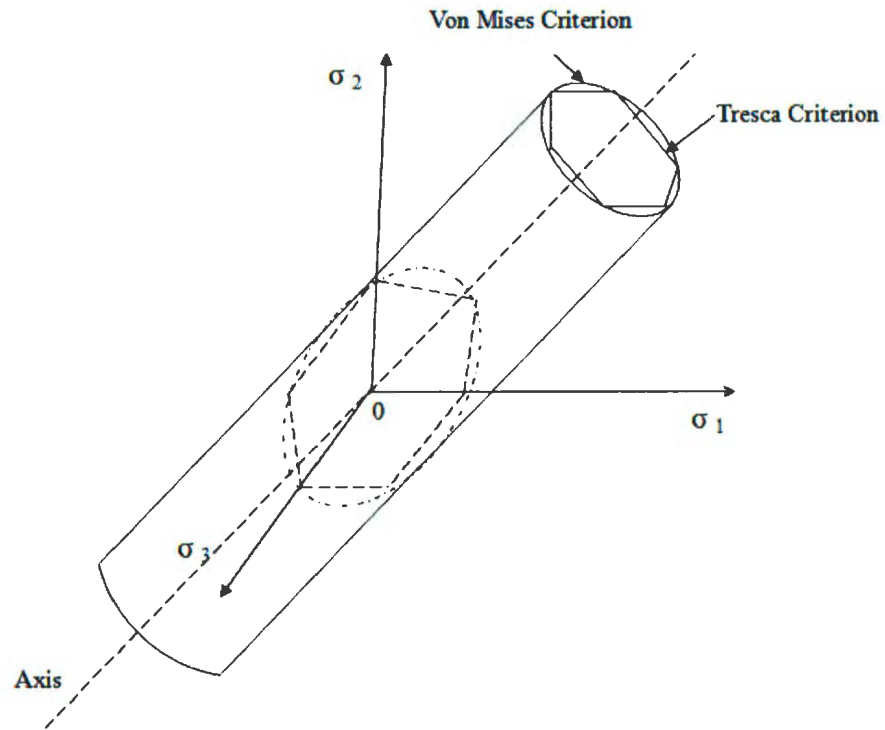


Figure 3.2 Yield Surfaces [34]

The yield locus is the boundary of the elastic zone in three-dimensional stress space.

### 3.3 THEORETICAL CONSIDERATIONS

Limit analysis plays an important role in design and integrity assessment of mechanical components and structures. Limit load is the load at which uncontained plastic flow (plastic deformation) occurs in a perfectly plastic structure, and the structure is on the verge of collapse. The estimation of limit load for mechanical components

provide a better means of structural integrity assessment and fitness-for-service evaluation. Limit analysis is especially attractive as it simplifies the inelastic analysis by assuming an elastic perfectly plastic material model.

Lower bound limit load is the load that a structure is able to carry safely during its service life and there is no permanent deformation of the structure. Lower bound limit load is attractive as it provides accurate margin of safety against load controlled plastic failure modes. The exact limit load multiplier is available only by performing a plastic limit analysis. Several estimates and bounds of the exact limit load multiplier can be obtained from an elastic analysis.

### **3.3.1 Classical Lower Bound Multiplier**

The lower bound multiplier can be directly obtained by applying the lower-bound theorem of plasticity. Assuming that some stress distribution throughout the component or structure can be found, which is everywhere in equilibrium internally, balances the external loads and at the same time does not violate the yield condition. Then the corresponding applied loads will be less than or equal to the exact limit load, and will be carried safely by a sufficiently ductile material. If  $\sigma_y$  is the yield strength of the elastic-perfectly plastic material, then the classical lower bound multiplier ( $m_L$ ) can be expressed as

$$m_L \approx \frac{\sigma_y}{\sigma_{\max}}; P_L = P m_L \quad (3.5)$$

where,  $P$  is the applied load and  $P_L$  is the limit load.

Statically admissible stress distributions can be constructed by “inspection”, or by using a closed form linear elastic solution. When a finite element analysis is performed, the stress distribution inside each element is approximate. Therefore,  $m_L$  obtained from linear elastic FEA is only a mesh-dependent estimate that is expected to converge to the exact value as the mesh is refined successively.

### 3.3.2 Upper Bound Multiplier

In classic limit analysis, the statically admissible stress field (equilibrium set) can not lie outside the yield surface and the stress associated with a kinematically admissible strain rate field (compatibility set) in calculating the plastic dissipation should lie on the yield surface. Mura et al. proposed an approach that eliminates such a requirement and replaced it by the concept of *integral mean of yield* based on a variational formulation. The integral mean of yield criterion can be expressed as,

$$\int_{V_T} \mu^0 \left[ f(s_{ij}^{-0}) + (\varphi^0)^2 \right] dV = 0 \quad (3.6)$$

where,  $\bar{s}_{ij}^0$  is the statically admissible deviatoric stress for impending plastic flow;  $\varphi^0$  is a point function which takes on a value of zero if  $\bar{s}_{ij}^0$  is at yield and remains positive below yield. The flow parameter  $\mu^0$  is defined through the associated flow rule as,

$$\dot{\epsilon}_{ij} = \mu \frac{\partial f}{\partial s_{ij}} \quad (3.7)$$

where,  $\mu^0 \geq 0$  (statically admissible set) and  $\dot{\epsilon}_{ij}$  is the strain rate. Now,  $\bar{s}_{ij}^0 = m^0 s_{ij}^0$  where  $s_{ij}^0$  corresponds to the applied traction,  $T_i$ . The von Mises yield criterion can be expressed as,

$$f(\bar{s}_{ij}) = \frac{3}{2} \bar{s}_{ij} \bar{s}_{ij} - \sigma_y^2 \quad (3.8)$$

Assuming an unspecified but constant flow parameter  $\mu^0$  and performing the necessary mathematical manipulations Eq. (3.8) becomes [6],

$$m^0 = \frac{\sigma_y \sqrt{V_T}}{\sqrt{\int_{V_T} (\sigma_{eq})^2 dV}} ; \varphi^0 = 0 \quad (3.9)$$

where,  $\sigma_{eq}$  is the von Mises equivalent stress and  $V_T$  is the total volume. Proof of the upper-boundedness of  $m^0$  is presented in Reinhardt and Seshadri [11]

### 3.3.3 The $m_\alpha$ Multiplier

The  $m_\alpha$  multiplier method [6] was developed on the basis of variational concepts in plasticity. The method has explicit dependency on the upper bound multiplier,  $m^0$ , and the classical lower bound multiplier,  $m_L$  and can be expressed as

$$m_\alpha = 2m^0 \frac{2\left(\frac{m^0}{m_L}\right)^2 + \sqrt{\frac{m^0}{m_L} \left(\frac{m^0}{m_L} - 1\right)^2 (1 + \sqrt{2} - \frac{m^0}{m_L}) \left(\frac{m^0}{m_L} - 1 + \sqrt{2}\right)}}{\left(\left(\frac{m^0}{m_L}\right)^2 + 2 - \sqrt{5}\right) \left(\left(\frac{m^0}{m_L}\right)^2 + 2 + \sqrt{5}\right)} \quad (3.10)$$

The issue of lower-boundness of  $m_\alpha$  has been discussed by Reinhardt and Seshadri [11]. Rewriting the expression for  $m_\alpha$  by normalizing with the as yet undetermined exact multiplier ( $m$ ), the following equation can be obtained:

$$R_\alpha = 2R^0 \left[ \frac{2\zeta^2 + \sqrt{\zeta(\zeta-1)^2(1+\sqrt{2}-\zeta)}(\zeta-1+\sqrt{2})}{(\zeta^2+2-\sqrt{5})(\zeta^2+2+\sqrt{5})} \right] \quad (3.11)$$

Where  $\zeta = m^0/m_L$ ,  $R_0 = m^0/m$ , and  $R_\alpha = m_\alpha/m$ .

Due to normalization,  $R_a = 1$  represents the boundary between the upper bound ( $R_a > 1$ ) and lower bound ( $R_a < 1$ ), as shown in Fig 3.3. The value of  $m_a$  becomes imaginary when  $m^0/m_L > 1 + \sqrt{2}$ , as would be the case for components with notches and cracks.

In Eq. 3.11, the exact multiplier ( $m$ ) for a component being analyzed is generally unknown. As well,  $m^0/m_L$ , which is equal to  $((\sigma_e)_{\max}/\sigma_{\text{ref}})$ , is a measure of the theoretical stress-concentration factor of the notch.

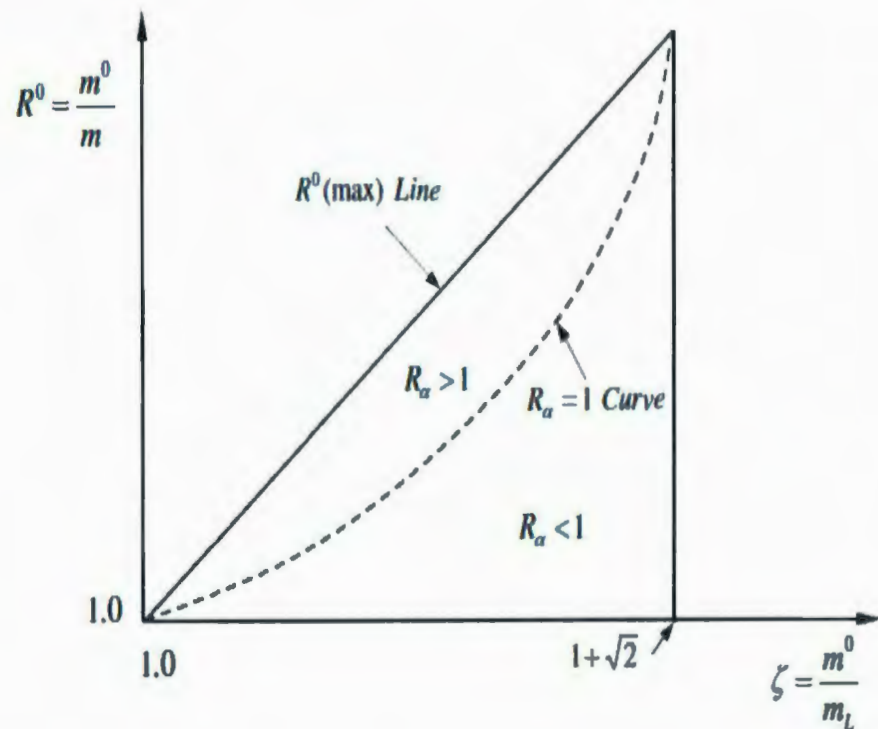


Figure 3.3 Regions of lower and upper bounds of  $m_a$  [13]

The region bounded by  $m^0(\max)$ ,  $1 \leq m^0/m_L \leq 1+\sqrt{2}$ , and  $1 \leq m^0/m \leq 1+\sqrt{2}$  is designated as the  $m_\alpha$  triangle.

### 3.3.4 The $m_\alpha$ – Tangent

The  $m_\alpha$  multiplier method [6] was developed on the basis of variational concepts in plasticity. The method has explicit dependency on the upper bound multiplier  $m^0$  and the classical lower-bound multiplier  $m_L$ . The upper bound multiplier,  $m^0$ , depends on the entire stress distribution in a component or structure whereas  $m_L$  depends on the magnitude of maximum stress. Therefore, for components with sharp notches and cracks, the value of  $m^0/m_L$  will be high due to the presence of peak stresses.

With respect to figure 3.4, the following can be stated:

- (1) When  $m$  approaches  $m_L$ , the domain of statically admissible  $m^0$  is bounded by the 45-degree ( $R^0(\max)$ ) line and the positive x-axis.
- (2) When  $m$  approaches  $m^0$ , the domain of statically admissible  $m^0$  is represented by the line  $m = m^0$ .
- (3) The exact solution ( $m$ ) locus would lie somewhere between the positive x-axis and the 45-deg line ( $R^0(\max)$ ).

- (4) The tangent to the  $R_\alpha=1$  curve at the limit state ( $m_l = m^0 = m$ ) will locate the  $m_\alpha$ -tangent, which can then be used to estimate the multiplier  $m$ .

The determination of the  $m_\alpha$ -tangent is as follows. Equation (3.10) can be represented by a curve in two dimensional space, as shown in Fig. 3.3. The slope of the tangent at the limit state, where  $m_\alpha=m^0=m_l=m$ , can be obtained as

$$\left. \frac{dR_\alpha}{d\zeta} \right|_{\zeta=1} = 1 - \frac{1}{\sqrt{2}} \quad (3.12)$$

Therefore, the slope of the tangent ( $R_\alpha^T = 1$ ) line at the converged limit state is

$$\tan(\theta) = 0.2929$$

The equation corresponding to  $R_\alpha^T = 1$  can be obtained as

$$\frac{m^0}{m} = 1 + (\zeta - 1)\tan(\theta) \quad (3.13)$$

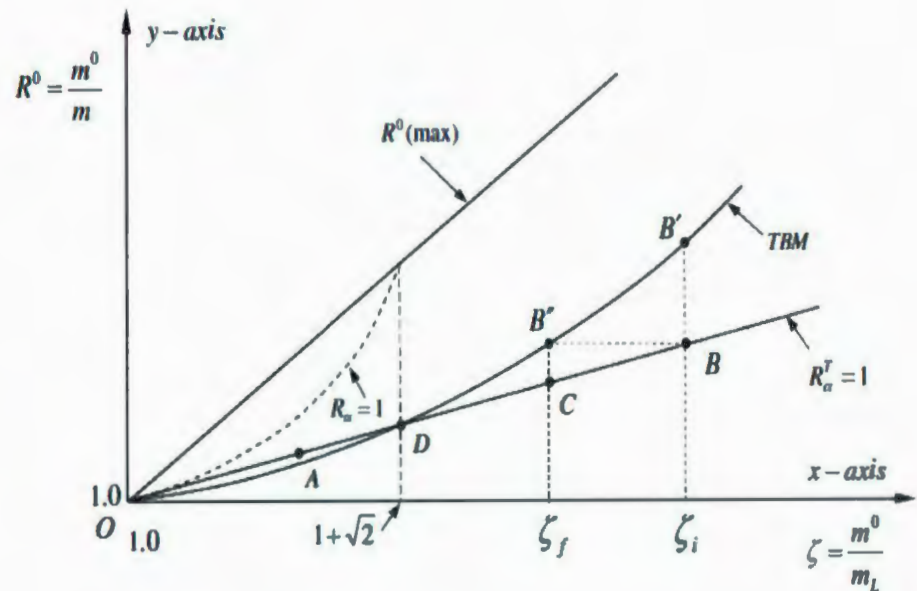


Figure 3.4 The  $m_\alpha$ -tangent construction [13]

The exact limit load multiplier ( $m$ ) for most of the practical components and structures being analyzed is not known a priori. For the  $m_\alpha$ -tangent method,  $R^0$  can be defined by making use of the tangent ( $R_\alpha^T$ -line in Fig. 3.3) for any value of  $\zeta$ . Both  $R^0$  and  $\zeta$  are greater than 1, except at the limit state for which  $R^0 = \zeta = 1$ . It should be noted that the reduction in  $m^0$  along the  $R_\alpha^T = 1$  trajectory implicitly accounts for the reference volume. Therefore,  $m^0$  will converge to the exact multiplier as the trajectory approaches the origin.

### 3.3.5 Blunting of Peak Stresses

Secondary and peak stresses are set up by redundant kinematic constraints (or static indeterminacy) in a component. ASME Boiler and Pressure Vessel codes [21, 22] explicitly recognize these stresses and related constraint effects. Figure 3.5 shows the stress distribution in the ligament adjacent to the notch tip, where x-axis represents the distance ahead of the notch tip, and y-axis is the equivalent stress.

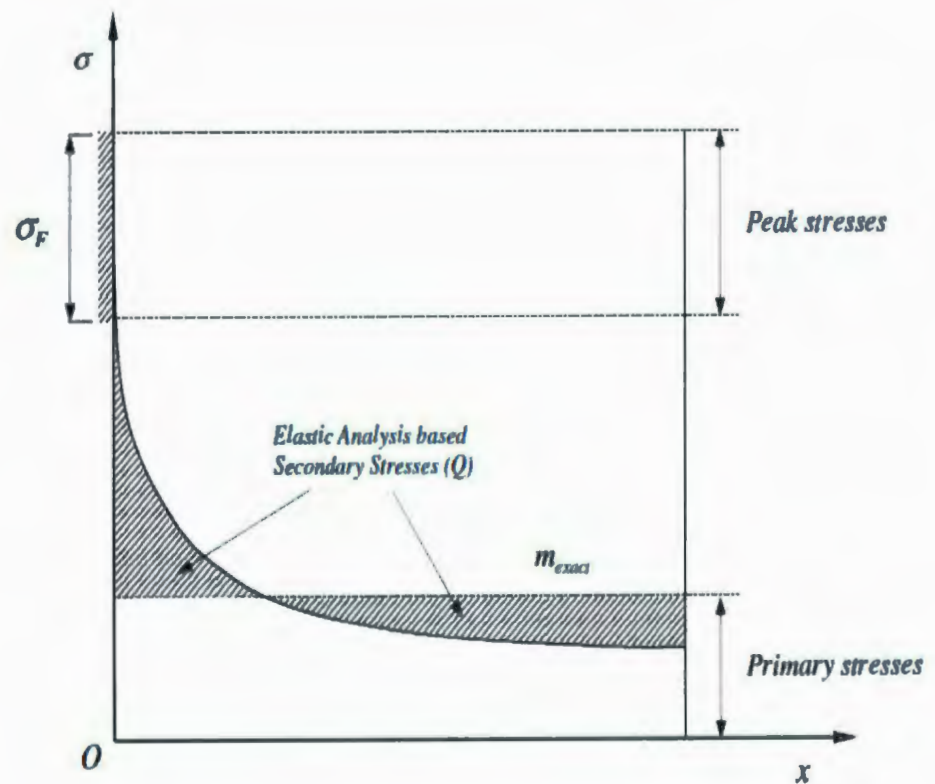


Figure 3.5 Stress distribution ahead of notch tip [13]

As can be seen from this figure, the magnitude of the equivalent peak stress ( $\sigma_F$ ) at the notch tip is considerably high; however, it is assumed that the peak stresses are very localized and that the following expression is valid

$$\int_A \sigma_F dA \approx 0 \quad (3.14)$$

Where  $A$  is the representative area on which  $\sigma_F$  acts.

With respect to the constraint map  $R_\alpha^T = 1$  line can be identified, as shown in Figure

3.4. This line is tangential to the  $R_\alpha^T = 1$  curve at the origin ( $m^0/m=1, m^0/m_t=1$ ).

### 3.3.6 Significance of $\zeta^* = 1 + \sqrt{2}$

The point D (Figure 3.4) can be determined by finding the intersection of the  $R_\alpha^T = 1$  line and the reference two-bar model [23] equation, that is,

$$\frac{m^0}{m} = 1 + (\zeta - 1) \tan(\theta) = \frac{1 + \lambda}{2\sqrt{\lambda}}$$

$$\text{Where } \lambda = \frac{1}{\zeta^2} \text{ and } \tan(\theta) = 1 - \frac{1}{\sqrt{2}} \quad (3.15)$$

The intersection points work out to be  $\zeta^* = 1.0$  and  $1 + \sqrt{2}$ . The  $R_\alpha^T = 1$  line represents a combination of primary and secondary stresses that exist in the pressure components.

### 3.3.7 The $m_\alpha$ -Tangent Method

Once the  $R_\alpha^T = 1$  line is identified, the  $m_\alpha^T$  value can be readily estimated by the relationship

$$m_\alpha^T = \frac{m^0}{1 + 0.2929(\zeta - 1)} \quad (3.16)$$

$$\zeta = \frac{m^0}{m_t}$$

The slope of the  $R_\alpha^T = 1$  line is equal to the  $\tan(\theta) = (1 - 1/\sqrt{2})$ . The value of  $m^0$  and  $\zeta$  can be determined from statically admissible distributions obtained from linear elastic FEA.

Two cases are considered next.

*Case 1:*  $\zeta \leq 1 + \sqrt{2}$ , *negligible peak stresses*. For this case, point A (Figure 3.4) is assumed to lie on the  $R_\alpha^T = 1$  line. The value of the  $m_\alpha^T$  can be obtained from equation (3.16). This case usually applies to well-designed pressure components with gentle geometric transitions.

*Case 2:*  $\zeta > 1 + \sqrt{2}$ , *presence of peak stresses*. This case applies to well-designed components that develop flaws or cracks in service or to components with sharp notches. The aim here is to blunt the peak stresses prior to evaluating  $m_\alpha^T$ .

With respect to Figure 3.4, the initial linear elastic FEA locates point B on the  $R_\alpha^T = 1$  line and point B' on the TBM [23] locus corresponding to  $\zeta_i = m_i^0 / m_{l,i}$ . The subscript  $i$  refers to the initial point  $B$  and  $B'$ . The calculation procedure is as follows.

1. Perform a linear elastic analysis.
2. Locate points  $B$  and  $B'$ . Point  $B$  represents the combination of primary and secondary stresses whereas point  $B'$  represents the combination of primary, secondary, and peak stresses.
3. Construct a horizontal line from points  $B$  to  $B''$  signifying an invariant  $m_i^0$  (blunting of peak stresses). Designate the value of  $m^0/m_l$  at  $B''$  as  $\zeta_f$ , which can be obtained by solving the following equation:

$$\frac{m_i^0}{m} = 1 + 0.2929(\zeta_i - 1) = \frac{\zeta_f^2 + 1}{2\zeta_f} \quad (3.17)$$

The roots of equation (3.17) are

$$\zeta_f = (1 + C) \pm \sqrt{(1 + C)^2 - 1} \quad (3.18)$$

Where  $C = 0.2929 (\zeta_i - 1)$

4. The value of  $m_\alpha^T$  can be evaluated by the equation [13]

$$m_\alpha^T = \frac{m_i^0}{1 + 0.2929(\zeta_f - 1)} \quad (3.19)$$

For some geometric transitions for which  $\zeta > 1 + \sqrt{2}$ , redistribution secondary stresses could occur along with peak stresses. In such cases, the value of  $m_i^0$  is not constant during the blunting of peak stresses, and there is a gradual reduction in its magnitude. These cases are usually attributed to components undergoing highly localized plastic flow such as beams and frame structures.

### 3.4 REMAINING STRENGTH FACTOR (RSF)

The remaining strength factor (RSF) proposed by Sims et al. [12] is used as a basis for the evaluation of thinned areas in pressure vessels and storage tanks. It is a dimensionless parameter and is based on the primary load carrying capacity of the structure. The RSF of a component containing damage is computed as the ratio of the strength of the damaged component to that of the component before damage. The remaining strength factor is defined as:

$$RSF = \frac{L_{dc}}{L_{uc}} \quad (3.20)$$

where

$L_{dc}$  = Limit or plastic collapse load of the damaged component (Component with flaws), and

$L_{uc}$  = Limit or plastic collapse load of the undamaged component

For tankage, the RSF acceptance criteria is [32]:

$$MFH_r = MFH (RSF/RSF_a) \quad \text{for } RSF < RSF_a \quad (3.21)$$

$$MFH_r = MFH \quad \text{for } RSF \geq RSF_a \quad (3.22)$$

where

$RSF$  = Remaining strength factor computed based on the flaw and damage mechanism  
in Component

$RSF_a$  = Allowable remaining strength factor

$MFH_r$  = Reduced permissible maximum fill height of the damaged tank course, and

$MFH$  = Maximum fill height of the undamaged component

If the calculated RSF is higher than the allowable RSF, the component is safe for operation. The recommended value for the allowable Remaining Strength Factor is 0.90 for equipment in process services [1]. This value may be reduced based upon the type of loading (e.g. normal operating loads, occasional loads, short-time upset conditions) and/or the consequence of failure.

The von Mises yield criterion can be expressed as

$$f(s_{ij}) = (m_d^0 \sigma_e)^2 - \sigma_y^2 = 0 \quad (3.23)$$

where  $m_d^0$  is the statically admissible multiplier for the damaged component,  $\sigma_e$  is the statically admissible equivalent stress, and  $\sigma_y$  is the yield stress. For components containing corrosion damage, the integral mean of yield using von Mises criterion can be expressed by integration of Eq. (3.6) as

$$[(m_d^0 \sigma_{eU})^2 - \sigma_y^2] V_U + [(m_d^0 \sigma_{eD})^2 - \sigma_y^2] V_D = 0 \quad (3.24)$$

where suffix  $U$  refers to the uncorroded region of the reference volume and suffix  $D$  refers to the corroded region,  $\sigma_{eU}$  is the equivalent stress in the original shell and  $\sigma_{eD}$  is the equivalent stress in the corroded area of the shell. Rearranging Eq. (3.24), we can obtain

$$m_d^0 = \sqrt{\frac{\sigma_y^2 V_R}{\sigma_{eU}^2 V_U + \sigma_{eD}^2 V_D}} \quad (3.25)$$

Three RSFs are considered next for evaluation of industrial storage tanks containing corrosion damage.

### 3.4.1 RSF Based on the Upper Bound Multiplier

The remaining strength factor  $RSF_U$  is based on the integral mean of yield criterion, along with the von Mises failure criterion. The upper bound  $RSF_U$  is obtained using  $m_d^0$  as

$$RSF_t = \frac{m_d^0}{m_u^0} \quad (3.26)$$

where  $m_u^0 = \sigma_y / \sigma_{eU}$  is the upper bound multiplier for the undamaged shell, and  $m_d^0$  is obtained from the integral mean of yield criterion. Since  $RSF_U$  is the ratio of an upper bound multiplier of a damaged component to that of the component in the undamaged condition, the RSF will be an upper bound estimate.

### 3.4.2 RSF Based on the $m_\alpha$ -Tangent Multiplier

The second *RSF* is obtained by using the  $m$ -alpha tangent multiplier ( $m_\alpha^T$ ), proposed by Seshadri and Hossain [13]. The  $m$ -alpha tangent multiplier based on Eq. (3.10), as described in section 3.3.6 of this thesis, can be used to calculate the RSF as follows

$$RSF^T = \frac{m_\alpha^T}{m_u^0} \quad (3.27)$$

While using Eq. (3.16) in order to evaluate  $RSF^T$ , the classical lower bound multiplier can be obtained as  $m_L = m_{Ld} (= \sigma_y / \sigma_{eD})$  and the upper bound multiplier  $m^0$  is equal to  $m_d^0$  as defined in Eq. (3.25).

### 3.4.3 RSF Based on Classical Lower Bound Multiplier

The third remaining strength factor  $RSF_L$  is based on the classical lower bound limit load multiplier  $m_L$  and is given by,

$$RSF_L = \frac{m_{Ld}}{m_u} \quad (3.28)$$

where the classical lower bound multiplier  $m_{Ld} = \sigma_y / \sigma_{eD}$  for corrosion damage. This RSF gives very conservative estimation of the assessment. The above mentioned RSFs are also used in this current research for FFS evaluation of storage tanks containing corrosion damage.

### **3.5 INELASTIC FINITE ELEMENT ANALYSIS**

The finite element method is a numerical technique, which can be applied for a wide range of engineering structures. Generally, engineering structures are complex in geometry and loading. Such problems are mathematically complex to be solved by classical analytical methods. FEA is a discrete analysis technique in which a large structure is divided into a number of simpler regions for which approximate solutions are easily obtainable. The procedure results in a large number of simultaneous algebraic equations, which are effectively, solved using a computer.

Non-linear finite element methods make inelastic analysis a viable approach for many engineers with the recent advancements in computer technology. If non-linear analysis can be performed, application of code rules is considerably simpler than the elastic stress categorization approach. Inelastic analysis is often performed using commercially available software packages (ANSYS, ABAQUS)

It is easier to solve structures with linear elastic behavior rather, than those experiencing inelastic deformation. In linear elastic analysis, the load-displacement relationship is linear. The problem is solved in a single-stage solution procedure. In inelastic analysis, the load-displacement relationship is nonlinear and therefore, the total load is applied in increments. The problem is solved in iterative manner, and is based on a

piece wise linear or incremental solution method. For each load increment, the stiffness matrix is updated to take account of changes in material properties of the elastic-plastic region. Moreover, each load step must satisfy certain convergence criteria, thereby balancing the calculated internal forces and moments and applied load.

Inelastic FEA is elaborate and provides considerable information about the structural behavior between the yield stress and collapse state of the structure. The analysis is complex and requires greater computing resources in order to perform several iterations to find the equilibrium displacements of load increments and store the intermediate data.

However, the non-linear FEA poses certain drawbacks. The definition of material models and the control of load increments to define the material properties have to be done precisely. Knowledge of available non-linear techniques is mandatory to achieve convergence. Convergence failure occurs for the load steps when the plasticity spread is significant and near collapse states thereby underestimating the limit loads. Selection of appropriate element and its mesh density greatly affects the inelastic analysis results. The designer's experience and expertise also plays a major role in deciding the solution control process.

In this current research Level 3 inelastic RSF is evaluated to verify the Level 2 RSFs obtained from the proposed analytical and linear elastic FEA based methods. Appropriate strain limits are used to obtain the collapse load of the structure. Sims et al. (1992) proposed a conservative limit on the amount of plastic strain in LTA based on numerous inelastic FEA. They argued that a limit of 2% plastic strain at any location provides a reasonable and conservative estimate of the actual collapse load of the structure. In the present work, 1% plastic strain at the middle fiber of any location in the LTA is considered as the limit for plastic collapse load estimation. The approach is consistent with the work reported in [5, 7, 8, 10] on FFS assessment of thermal hot spots and corrosion damage.

### **3.6 HYDROSTATIC PRESSURE ON LIQUID STORAGE TANKS**

Liquid storage tanks experience differential pressure on the vertical wall of the tank due to the hydrostatic head. Pressure vessels and piping systems generally experience uniform pressure. In order to apply the concept of decay lengths and reference volume, originally derived for pressure vessels and piping subjected to uniform internal pressure, equivalent hydrostatic pressure needs to be calculated for the kinematically active volume.

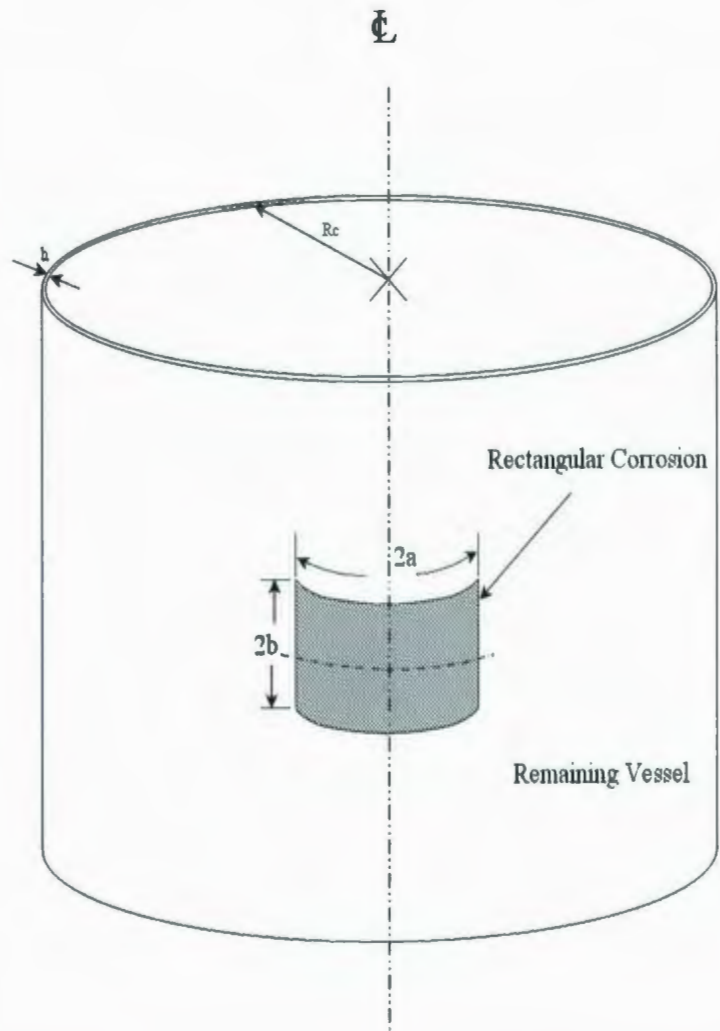


**Fig. 3.6** A schematic diagram of rectangular LTA in a storage tank

Since the pressure varies with depth, the variation can be represented by Figure 3.7, where the pressure is equal to zero at the upper surface and equal to  $\gamma H$  at the bottom and  $\gamma$  is the specific weight of liquid.

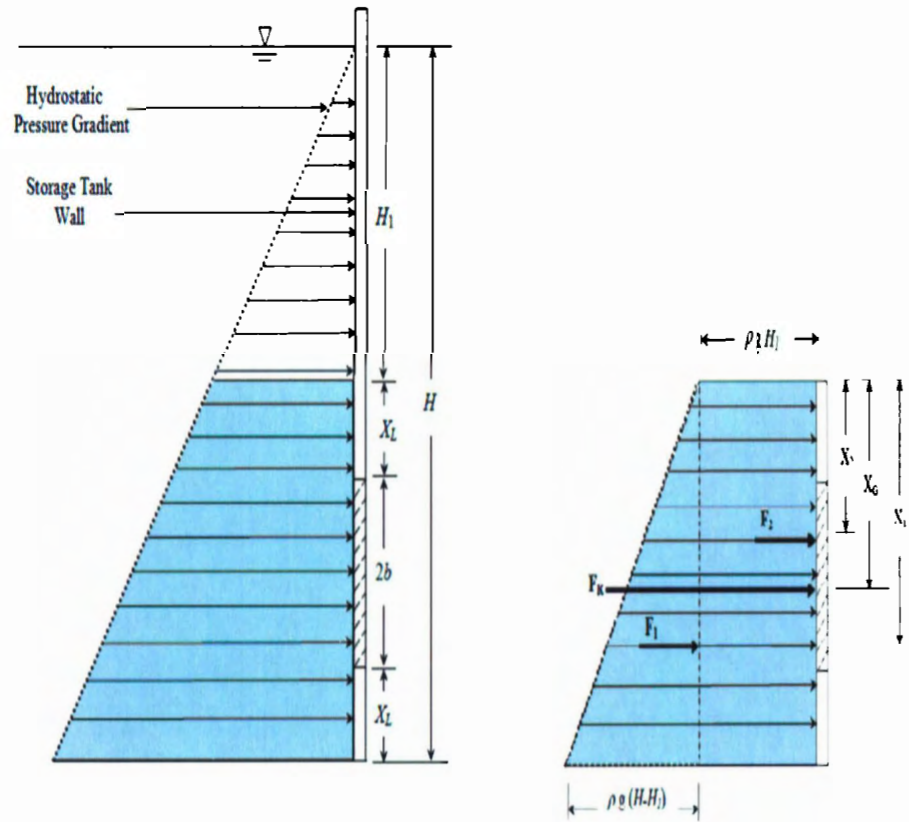


Fig 3.7 Graphical representations of hydrostatic forces on a vertical rectangular surface

With respect to figure 3.7, equivalent hydrostatic pressure on the LTA is evaluated using the following equation:

$$P_{eqv} = \bar{X}_G \rho g, \quad (3.29)$$

$$\text{where } \bar{X}_G = \frac{(A_1 X_1 + A_2 X_2)}{A_1 + A_2} \quad (3.30)$$

For calculating the equivalent hydrostatic pressure the total area of the reference volume LTA where the hydrostatic pressure acting is divided into two regions as shown in Fig. 3.7 For triangular region centroid lies at one third of its height from the base and for rectangular region it lies at half of height from the base. Equivalent distance  $\bar{X}_G$  is the vertical distance from the fluid surface to the centroid of the LTA. Equivalent distance ( $\bar{X}_G$ ) is obtained by using the centre of gravity for triangular ( $X_1$ ) and rectangular ( $X_2$ ) profiles and their respective areas.

The current approach to find the equivalent distance is consistent with the work reported by Munson et al [16] to evaluate the location of the resultant force on a cylindrical oil storage tank. Equivalent pressure ( $P_{eqv}$ ) on LTA is calculated using equivalent distance ( $\bar{X}_G$ ), density of liquid ( $\rho$ ) and gravitational acceleration ( $g$ ).

### 3.7 CLOSURE

A review of the theory of plasticity, classical lower bound multiplier, upper bound multiplier,  $m_a$  method and the  $m_a$ -tangent multiplier method has been undertaken in this chapter. Three remaining strength factors exercised in the current study are based on classical lower bound multiplier,  $m_a$ -tangent multiplier and upper bound multiplier. These remaining strength factors are employed in chapter 5 to evaluate the RSF of a liquid storage tank containing corrosion damage. Level 3 inelastic finite element analysis is discussed briefly in this chapter, as it is used in this current research to validate the results obtained from the proposed methods. This chapter also presents the procedures for evaluating the equivalent hydrostatic pressure on liquid storage tanks containing corrosion damage. The application of the  $m_a$ -tangent multiplier to evaluate the remaining strength factor of a liquid storage tank with corrosion damage will be presented in chapter 4.

## **CHAPTER 4**

### **FITNESS FOR SERVICE (FFS) PROCEDURE**

#### **4.1 INTRODUCTION**

Integrity assessment of mechanical components and structures is a multidisciplinary effort. Structural integrity is of considerable interest in many industrial sectors e.g., oil and gas, nuclear, and petrochemical industries. Integrity assessment is considered an essential tool in order to ensure the safety and economy of an operating plant. Fitness-for-service (FFS) assessments are performed in order to demonstrate the structural integrity of mechanical components and structures undergoing damage. FFS assessment also aids in optimal maintenance and operation of the plants. In practice, FFS evaluations are conducted periodically in order to assess the acceptability of the components for continued service as well as to estimate the remaining life of the components or structures. Recommended practices and procedures associated with FFS assessment are API 579 [1], R6 [2], SINTAP [3], and RSTRENG [4]. For pressurized equipments in operating plants, API 579 has provided three levels of assessment.

## 4.2 EFFECTIVE AREA METHODS

The study of pressure vessels containing blunt metal-loss or corrosion damage, usually considered as a locally thinned area (LTA), has been far more elaborate compared to that for thermal hot spot problems. However, most studies are on the evaluation of piping and cylindrical vessels.

The ASME B31G, modified B31G and RSTRENG methods form a class of evaluation methods that replace the actual metal loss with an “effective” cross sectional area. The remaining pressure carrying capacity of the component i.e. pipeline or cylindrical vessels are calculated based on the amount and distribution of metal loss, and the yield strength of the component. Note that for crack-like defects and defects caused by stress corrosion cracking (SCC), the failure mechanism is based on material toughness and the evaluation procedures are different. SCC is cracking due to process involving conjoint corrosion and straining of a metal due to residual or applied stress . This requires specific combinations of metal and environment such as chloride cracking of stainless steel or hydrogen embattlement of high strength steels (Cottis, 2000). This type of corrosion is currently dealt with by Level 3 assessment according to API 579 [1] and is not of direct interest in the current research.

The effective area method was first developed from a semi-empirical fracture mechanics relationship by Maxey, et al. (1972). The method assumes that the strength loss due to corrosion is proportional to the amount of metal loss measured axially along the pipe (s). The remaining strength factor is based on a Dugdale plastic-zone-size model and a “Folias” factor. Folias factor is a bulging stress magnification factor used in through-wall crack in pressurized cylinder [12]. An empirical flaw-depth-to-pipe-thickness relationship is used to modify the Folias factor to account for part-through wall effects based on “effective” cross sectional area. This method assumes that the flaw fails when the stress in the flaw reaches the flow stress  $\sigma_{flow}$ . The nominal pipe wall hoop stress at failure in the flaw is given by

$$\sigma_{fail} = \sigma_{flow} \left[ \frac{1 - A/A_0}{1 - A/A_0 \{M^{-1}\}} \right] \quad (4.1)$$

Where,  $A$  is the corroded area in the cross section,  $A_0$  is the cross sectional area,  $M$  is Folias factor. The term in the bracket is proposed as the effects from effective area for a surface flaw.

#### 4.2.1 ASME B31G Criterion

The expression for nominal hoop stress at failure  $\sigma_{fail}$  of a flaw used by ASME B31G [9] is

$$\sigma_{fail} = 1.1 \sigma_y RSF \quad (4.2)$$

$$RSF = \left[ \frac{1 - (2/3)(d/t)}{1 - (2/3)(d/t)(M^{-1})} \right] \quad (4.3)$$

where,  $\sigma_y$  is the yield stress,  $d$  is the maximum depth of corrosion and  $t$  is the pipe thickness. The Folias factor, used in this assessment is a function of the corrosion axial length  $s$ , the pipe diameter  $D$ , and  $t$  as

$$M = \sqrt{1 + 0.8 \left( \frac{s^2}{Dt} \right)} \quad (4.4)$$

It can be observed by comparison of Eq. (4.1) and (4.2) that this method assumes that flow stress  $\sigma_{flow} = 1.1 \sigma_y$ . The flow stress used in this method is conservative when compared with yield stress for cylinders calculated using von-Mises criterion with elastic-perfectly plastic model which is equal to  $2/\sqrt{3} \sigma_y$  or  $1.15 \sigma_y$ . The corrosion flow is assumed to have a parabolic shape and hence parameter  $A = 2/3 sd$  and  $A_0 = st$ . The two-

term form of the Folias bulging factor is used to simplify the calculation. However, this two-term is only applicable to flaws with  $s/\sqrt{RT} < 6.3$  and  $d/t \geq 0.175$ . Beyond this length, the flaw depth is limited to 10 percent of the wall thickness. This limitation in a discontinuity in the flaw assessment criterion that contributes frequently to excessively conservative evaluations of LTAs in pipelines

#### 4.2.2 Modified ASME B31G Criterion

The modified B31G criterion attempts to reduce B31G simplifying assumptions and associated conservatism. The modified B31G criterion is given by

$$\sigma_{fail} = (\sigma_y + 10,000 \text{ psi})RSF; \quad (4.5)$$

$$RSF = \left[ \frac{1 - (0.85)(d/t)}{1 - (0.85)(d/t)(M^{-1})} \right] \quad (4.6)$$

where,  $M = \sqrt{1 + 0.6275 \left( \frac{s^2}{Dt} \right) - 0.003375 \left( \frac{s^2}{Dt} \right)}$  for  $\left( \frac{s^2}{Dt} \right) \leq 50$  and

$$M = 0.032 \left( \frac{s^2}{Dt} \right)$$

$$\text{for } \left( \frac{s^2}{Dt} \right) > 50.$$

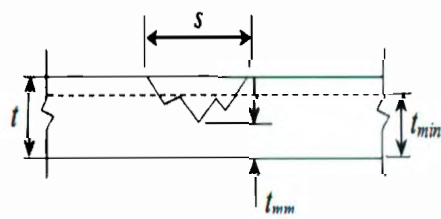
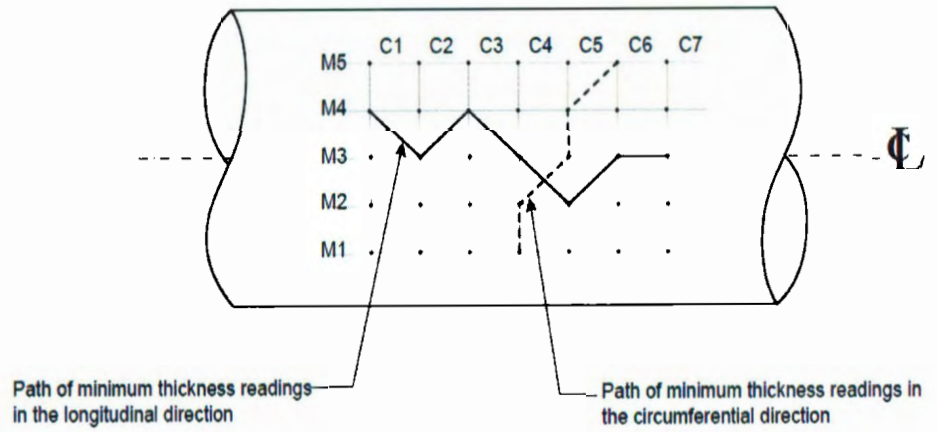
The flow stress used in Modified B31G is less conservative than B31G; for high strength pipeline material such as API 5L X80, the flow stress calculated by using Eq. (4.5) is  $1.125 \sigma_y$ . For lower strength material such as API 5L grade A, with a yield stress of 30000 psi, the flow stress becomes  $1.333 \sigma_y$ . This assumes that the material attains significant amount of strain hardening after yield. An empirical fit factor of 0.85 is also used in this criterion instead of the "2/3" area factor resulting from the assumed parabolic shape. In addition, the more accurate 3-term expression for the Folias bulging factor is utilized and hence the discontinuity that exists in B is eliminated.

#### 4.2.3 RSTRENG

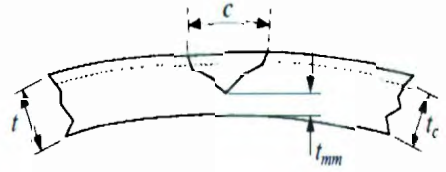
The more accurate computation of the effective area is developed by applying more detailed corrosion profiles with the help of PC-based software known as RSTRENG.

RSTRENG uses the less conservative definition of flow stress and the 3-term Folias bulging factor described in the Modified B31G. The equivalent axial profile can be made by plotting points along the deepest path of the contour map, often referred to as the critical thickness profile (CTP) or "river bottom" of the flaw (Figure: 4.1). RSTRENG computes the failure pressure based upon all possible flaw geometries along the river bottom and reports the lowest as its result. Although RSTRENG provides more accurate

results, difficulties can often arise because of a large amount of information must be collected.



(a) Longitudinal CTP



(b) Circumferential CTP

Figure 4.1 Procedure to establish the critical thickness profiles (CTP)

Note that the effective area method is a strength dependent method in which material toughness is not considered. Toughness is the ability of the material to withstand fracture. This implies the assumption of ductile material which is able to undergo large deformation before failure and the fracture is non-crack-like.

### **4.3 FITNESS-FOR SERVICE ASSESSMENT PROCEDURE**

Fitness-for-Service assessments are quantitative engineering evaluations that are performed to demonstrate the structural integrity of an in-service component containing flaw or damage. Three levels of assessment are presented by API 579 as given below:

Level 1: The assessment procedures included in this level are intended to provide conservative screening criteria that can be utilized with a minimum amount of inspection or component information. Level 1 assessment may be performed by either plant inspectors or engineering personnel.

Level 2: The assessment procedures included in this level are intended to provide a more detailed evaluation that produces results that are more precise than those from a Level 1 assessment. In a Level 2 Assessment, inspection information similar to that required for a

Level 1 assessment are needed; however, more detailed calculations are used in the evaluation. Level 2 assessments would typically be conducted by plant engineers, or engineering specialist's experienced and knowledgeable in performing FFS assessments.

Level 3: The assessment procedures included in this level are intended to provide the most detailed evaluation which produces results that are more precise than those from a Level 2 assessment. In a Level 3 assessment the most detailed inspection and component information are typically required, and the recommended analysis is based on numerical techniques such as the finite element method. A Level 3 analysis is primarily intended for use by engineering specialists experienced and knowledgeable in performing FFS assessments.

As mentioned previously, the current study aims at deriving Level 2 methods for FFS assessment of liquid storage tank experiencing hydrostatic pressure with corrosion damage. Evaluation procedures for cylindrical storage tanks are based on  $m_a$ -tangent multiplier, reference volume and variational principle.

#### 4.4 API 579 EVALUATION PROCEDURE

The metal loss in pressure vessels due to corrosion is divided into two main categories in API 579 (2000). The assessment procedure is classified as

- General Metal Loss Rules
- Local Metal Loss Rules

In order to distinguish between general metal loss and local metal loss, characteristics of the metal loss profile should be known in detail. The main difference between the assessment approaches of these two types of metal losses is that the amount of data that is required for the assessment. The general metal loss rules are based on the average depth of metal loss while the local metal loss rules are based on more accurate metal loss profiles, known as the critical thickness profiles (CTP's). Both general and local metal loss rules provide guidelines for Level 1 and Level 2 assessments. The present thesis focuses on the evaluation of local metal loss, which is generally termed as "locally thinned area" (LTA).

#### 4.4.1 Level 1 Assessment procedure from API 579

The API 579 assessment provides a consistent result for regions of metal loss with significant thickness variability (Osage, 2001). Two acceptance criteria are included; a simple level 1 criterion based on length and depth dimensions. Level 2 criterion is more complex based on the detailed cross-sectional profile. The assessment procedures for circumferential stress in pressure vessels with LTA subject to internal pressure are as shown below. The remaining thickness ratio,  $R_t$ , and the metal loss damage parameter,  $\lambda$ , are computed as

$$R_t = \frac{t_{mm} - FCA}{t_{min}} \quad (4.7)$$

$$\lambda = \frac{1.285L_m}{\sqrt{Dt_{min}}} \quad (4.8)$$

$t_{mm}$  is the minimum measured remaining wall thickness.

$t_{min}$  is the minimum required wall thickness in accordance with original construction code

$FCA$  Future Corrosion Allowance

$L_{msd}$  is the distance between the flaw and any major structural discontinuity

$L_m$  is the measured axial extent of corrosion

$D$  is the outer diameter of the cylinder

The stress at failure of LTA is computed as

$$\sigma_{fail} = \frac{\sigma_y \cdot RSF}{0.9} \quad (4.9)$$

$$RSF = \frac{R_t}{1 - (1 - R_t)M^{-1}} \quad (4.10)$$

where,  $M = \sqrt{1 + 0.48\lambda^2}$

The geometrical limitations on the region of local metal loss are

$$R_t \geq 0.20$$

$$L_{msd} \geq 1.8\sqrt{(Dt_{min})}$$

$$t_{min} - FCA \geq 2.5 \text{ mm, where } L_{msd} \text{ is the shortest distance between the}$$

edge of corrosion area and the discontinuity.

#### 4.4.2 Level 2 Assessment procedure from API 579

Level 2 assessment procedures can be used to provide a better estimation of the RSF (API 579, Sec 5.4.3). The inherent strength of the actual thickness profile is evaluated using an incremental approach to ensure that the weakest ligament is identified and properly evaluated. The limitations are stated in equations (4.1) and (4.2) are satisfied, and if  $\lambda \leq 5.0$ , then the RSF is computed for each of the subsections (Fig 4.2) of the critical thickness profile in both longitudinal and circumferential directions using the eq (4.10).

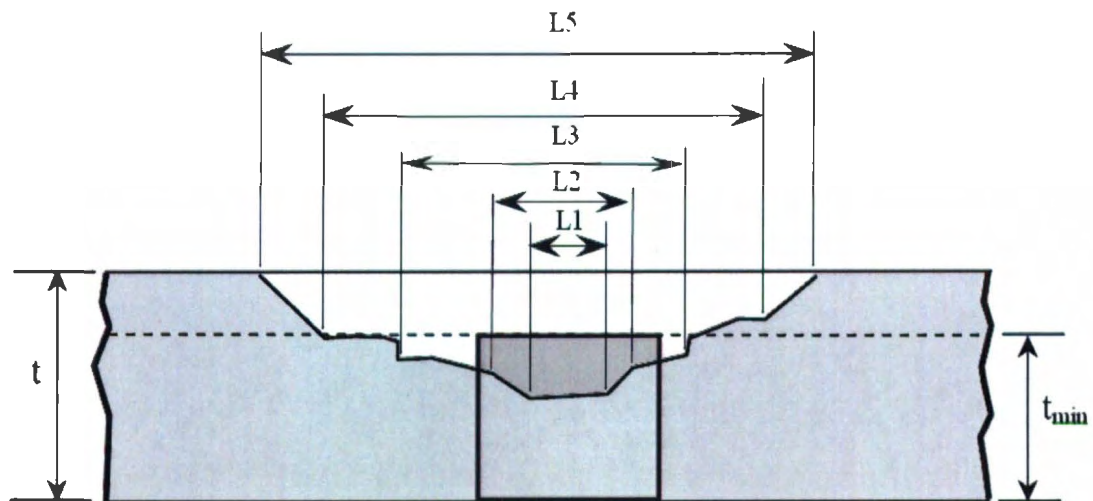


Figure 4.2 Subdivision process for Determining the RSF

$$RSF^i = \frac{1 - \frac{A^i}{A_o^i}}{1 - \frac{A^i}{A_o^i} M^{-i}} \quad (4.11)$$

where,  $A_o^i = L^i t_{min}$  is the original area based on  $L^i$

$$M^i = \sqrt{\frac{1.02 + 0.4411(\lambda^i)^2 + 0.006124(\lambda^i)^4}{1 + 0.02642(\lambda^i)^2 + 1.533(10^{-6})(\lambda^i)^4}} \quad (4.12)$$

where “i” corresponds to respective subdivision

The RSF calculated in this expression gives more accurate results due to the smaller size of the subsection.

#### 4.5 FACTORS INFLUENCING CORROSION FAILURE

An accurate FFS evaluation for a liquid storage tank having a corrosion spot is complex. A number of parameters affecting the behavior of the flaw and the failure of the component. From the experimental studies it is evident that the failure of corroded component can occur either by ductile failure (non crack-like flaws) or toughness dependent failure (crack-like flaws). This current study focuses on the non-crack-like corrosion in storage tanks.

In order to determine the strength of corroded components, corrosion damage is considered as locally thinned area (LTA). The applied loadings, geometry of the tank, corrosion profile and its material characteristics all drive the failure of the locally thinned area as shown in the Table 4.1.

Applied Loading	Geometry	Material Characteristics
Internal Pressure	<ul style="list-style-type: none"> <li>▪ Tank Dimensions               <ul style="list-style-type: none"> <li>- Diameter</li> <li>- Wall Thickness</li> </ul> </li> <li>▪ Defect Geometry               <ul style="list-style-type: none"> <li>- Depth</li> <li>- Length</li> <li>- Width</li> <li>- Shape/Profile</li> </ul> </li> </ul>	<ul style="list-style-type: none"> <li>▪ Yield Strength</li> <li>▪ Ultimate Strength</li> <li>▪ Fracture Toughness</li> <li>▪ Plasticity/Strain Hardening</li> <li>▪ Limiting Strain for acceptable performance</li> </ul>

Table 4.1 Factors influencing the behavior of LTA

The applied loads include the direct surface traction (internal pressure) and the net section tensile, compressive loads.

The overall schematic of the factors contributing to failure of LTA is illustrated in Figure 4.3 Failure occurs when the effect of driving forces which induce the stresses and strains exceeds the material resistance.

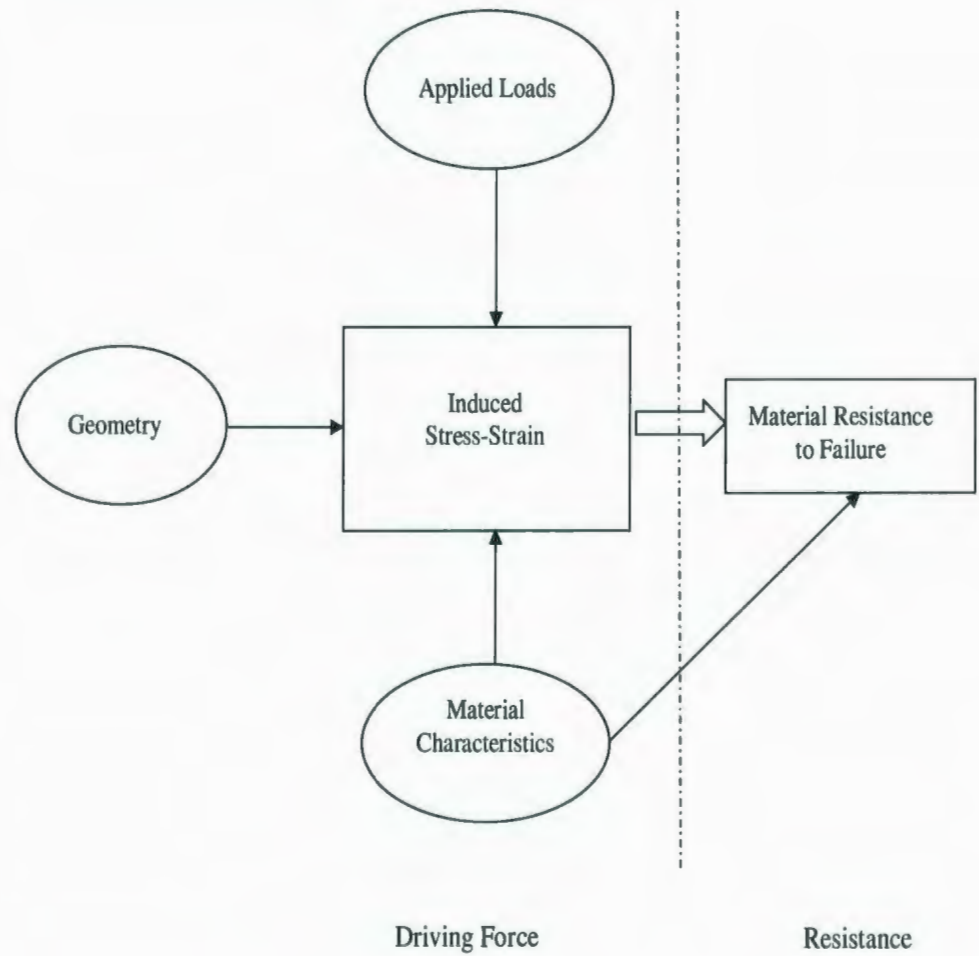


Figure 4.3 Schematic diagram of primary factors controlling the behavior of locally thinned areas [43]

#### 4.6 METHODOLOGY FOR PROPOSED LEVEL 2 FITNESS-FOR-SERVICE (FFS) EVALUATION FOR LIQUID STORAGE TANKS

In this current research, cylindrical liquid storage tank containing irregular profiles of flaws are represented by equivalent regular shapes to facilitate the evaluation procedures for remaining strength factor. A flaw profile is replaced by an equivalent rectangle enclosing the defect with the edges along circumferential and meridian directions of the shell as shown in the Figure 4.4

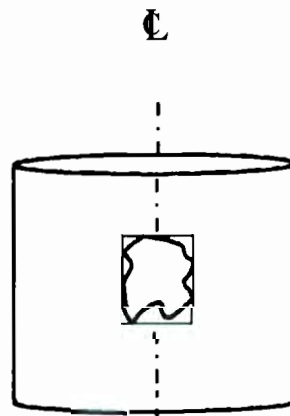


Figure 4.4 Rectangular Equivalent Area in Cylindrical Vessel

When corrosion damage occurs in a component with internal pressure, the damaged region undergoes higher deformation than the undamaged region. Excessive plastic deformation in a damaged area can lead to plastic collapse over a localized region of a component. The concept of reference volume has been introduced by Seshadri and Mangalaramanan [6]. This concept is to identify the kinematically active portion of the

structure that participates in plastic action. The reference volume prescribes the containment of effects of local stresses and strains acting on a structure. The current approach to find the Remaining Strength Factor (RSF) is consistent with the work reported by Tantichattanont et al. [17].

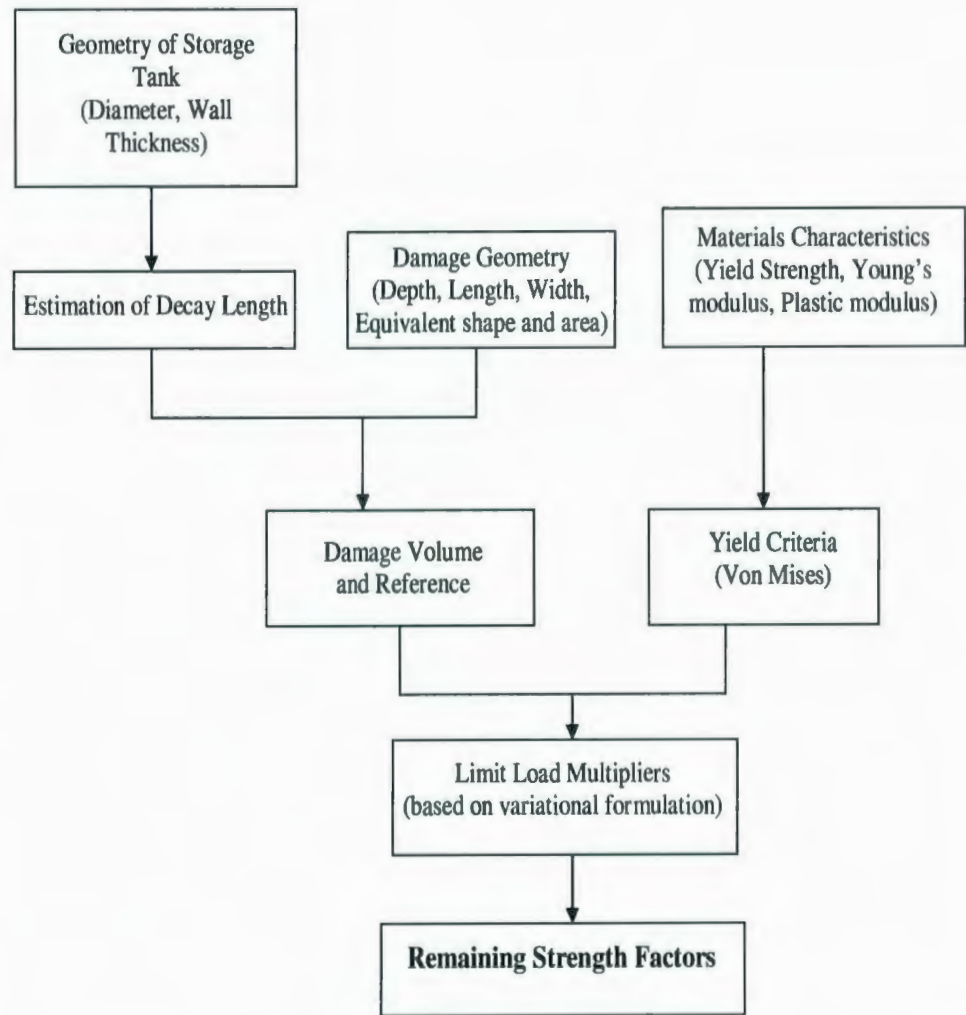


Figure 4.5 Contributing parameters to the proposed Level 2 evaluation methods [17]

## 4.7 DECAY LENGTH AND REFERENCE VOLUME

The concepts of decay length and reference volume has been discussed by Seshadri [5] in order to identify the kinematically active portion of the shell that takes part in plastic action. During local plastic collapse, the plastic action is assumed to occur in a localized region as shown in Fig. 4.6.

### 4.6.1 Decay Length

The localized effect of discontinuities due to corrosion damage in pressurized components is represented by introducing the concept of decay length. The decay length is defined as the distance from the applied force (or moment) to the point where the effect of the force is almost completely dissipated or becomes negligible. To deduce the expression for decay lengths in the axial direction, consider a cylindrical shell subjected to axisymmetric loading. In this case, the displacements are independent of the circumferential coordinate. For pressure vessels and piping, taking  $\nu = 0.3$ , the decay length in axial direction becomes [5]

$$x_l = 2.5\sqrt{Rh} \quad (4.13)$$

The decay length in circumferential direction for cylindrical shell can be calculated as [14]

$$x_c = 6.3\sqrt{Rh} \quad (4.14)$$

Since the extent of decay length in shells is dependent on shell curvature, the decay lengths in circumferential and axial directions are different. Justification of the decay lengths in cylindrical shells will be discussed in the following section.

#### 4.6.2 Reference Volume

When damage occurs in a pressurized component, a part of the volume, adjacent to the damage, participates in the failure mechanism. A reference volume is the sum of the volume of damaged portion of the vessel (LTA) and the adjacent volume affected by the damaged portion. The adjacent volume is the effective undamaged volume outside the damaged area that participates in plastic action and is part of the reference volume. The dimensions of the adjacent volume are calculated by using the decay lengths. An equivalent rectangular shape is utilized to represent an irregular shape of a corroded damage in cylindrical shells. Although the thickness of the corrosion is irregular in practice, generally a uniform depth is considered. Maximum corrosion depth is the conservative assumption. For a damaged area of width  $2a$  in circumferential direction and length  $2b$  in longitudinal direction of a cylindrical shell, as shown in Fig. 4.6, the volume of the damaged spot  $V_D$  can be calculated as,

$$V_D = 4abh_d \quad (4.15)$$

where,  $h_d$  is the thickness of the damaged area. The adjacent volume is the strip around the damaged volume that participates in plastic action and is bounded by decay lengths of cylindrical shells. Therefore, the adjacent volume is given by,

$$V_U = 4h((x_c + a)(x_l + b) - ab) \quad (4.16)$$

where,  $x_l$  and  $x_c$  are decay lengths of cylindrical shells in axial and circumferential directions, respectively. The reference volume is therefore the sum of the above volumes

$$V_R = V_D + V_U \quad (4.17)$$

where,  $V_D$  = Damaged Volume

$V_U$  = Undamaged Volume

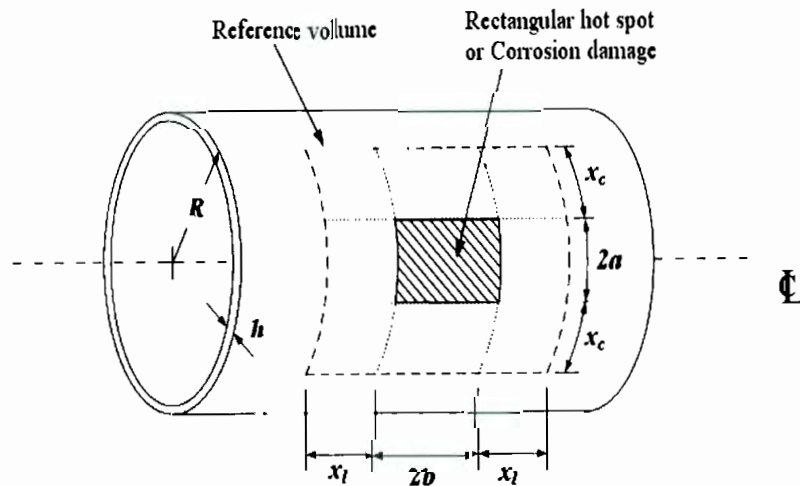


Figure 4.6 Decay length and reference volume dimensions for cylindrical shell

## 4.8 CLOSURE

Level 2 Fitness-for-Service assessment methods are developed to estimate the remaining strength factor of cylindrical liquid storage tanks with locally thinned areas. An overview of the existing Fitness-for-Service assessments of corrosion damage is presented. It is observed that there is a lack of procedures for evaluating RSF for liquid storage tanks experiencing hydrostatic pressure rather than constant pressure, containing corrosion damage.

The main factors influencing the behavior of pressurized components containing local damages such as corrosion damage, geometries of the damage and the shell and material characteristics are presented in this chapter. These major factors have been considered in the proposed Level 2 assessment based on the variational principle and the concept of reference volume. The reference volume identifying the volume participates in plastic action for cylindrical shells can be determined by using decay lengths of the shell.

## **CHAPTER 5**

### **APPLICATION TO CYLINDRICAL STORAGE TANK**

#### **5.1 INTRODUCTION**

Accurate structural analysis requires the concurrent satisfaction of the equilibrium equations, static boundary conditions, strain-displacement relations or compatibility conditions and kinematic boundary conditions. The stresses and strains are related by approximate material constitutive relationship; strain-displacement relations and equilibrium equations are independent of material property but have to satisfy both in the elastic and plastic range. The basic difference between elastic and inelastic analysis is the choice of material constitutive relationship, which is linear in elastic range and non-linear in plastic range. The satisfaction of compatibility conditions within the structure demonstrates the continuity of the structure in terms of the main degree of freedom, which is the displacement in structural analysis. In elastic range strains can be determined uniquely from the state of stress. In the inelastic range for determining the strains requires the knowledge of loading history. Conventional inelastic finite element analysis involves an iterative solution using the Newton-Raphson method.

In this chapter, a detailed parametric study of liquid cylindrical storage tank experiencing hydrostatic pressure having internal corrosion has been carried out. Indermohan and Seshadri [7] demonstrated the application of robust limit load solution for internally corroded pipeline with a radius to thickness ratio of greater than 50. Ramkumar and Seshadri [8] extended this work for a thicker pipeline having a radius to thickness ratio of about 30 with both internal and external corrosion. Tantichattanont et al. [10] have studied corrosion damage in spherical pressure vessels. Significant effort has been made towards the study of structural integrity of pressure vessels and piping systems undergoing damage. However, widespread research has not been reported in the area of structural integrity assessment of industrial storage tanks with locally thin areas (LTA). Sims et al. [12] have studied LTA in gas storage tanks in the context of FFS assessment. They have reported results of some parametric analysis using inelastic FEA, and have attempted to provide empirical equations for FFS assessment.

In this current thesis a typical liquid storage tank [20] experiencing hydrostatic pressure, and having internal corrosion damage, is chosen for the study. Two alternative methods based on statically admissible stress fields are proposed. The first method is a simple analytical approach, and the second method is based on two linear elastic finite element analyses. The proposed methods are shown to give a conservative assessment of the remaining strength of storage tanks containing local thin areas.

## 5.2 FINITE ELEMENT MODELING

In general, engineering structures are complex in geometry and loading. Such problems are mathematically complex to be solved by classical analytical methods. The finite element method is numerical technique, which can be applied for a wide range of engineering structures. FEA is a discrete analysis technique in which a large structure is divided into a number of simpler regions for which approximate solutions are expedient. The objective of the inelastic finite element analysis in this current work is to validate the solution obtained analytically, since NFEA remains the most accurate numerical solution that may be obtained for complex engineering problems.

Three-dimensional inelastic finite element analysis incorporating the effect of strain hardening was carried out using ANSYS [15]. Finite element models were created for simulating liquid storage tanks experiencing hydrostatic pressure containing internal corrosion damage. The metal loss in the storage tank due to corrosion is modeled by a reduced section thickness at the corrosion site, with other characteristic dimensions being longitudinal and circumferential extent of corrosion. Due to the difficulty of modeling highly irregular actual corrosion profiles, simplified regular rectangular and square profiles of corrosion were simulated. Half of the structure is modelled by taking advantage of symmetry.

A three-dimensional solid continuum finite element model was constructed using the eight noded brick SOLID 185 element. This element has 3 degrees of freedom per node (displacements in X, Y and Z directions). Four elements were used through the thickness in the corroded region. Since SOLID 185 element is linear element without mid-side nodes, an increased number of elements were needed to simulate the deformation behavior of the thinned area, and the discontinuity region between the corroded and uncorroded regions of the tank. The element has plasticity capability. Pressures may be input as surface loads on the element faces. Further, such a fine mesh prevents the occurrence of common meshing errors such as the error due to aspect ratio of the elements in the reference volume. All elements are automatically tested for acceptable shape in ANSYS.

### 5.3 MATERIAL MODEL

The material used in the current research is SA 516 Gr. 55, which is common carbon steel for pressure vessels. An elastic modulus of  $30 \times 10^6$  psi and a Poisson's ratio of 0.3 were used in the current research. Yield stress of 30,000 psi was used. The effect of strain hardening is included in this analysis to take advantage of the post-yield behavior of high strength steels. Accordingly, a representative bilinear material model with a plastic modulus of  $50 \times 10^4$  psi is used. Indermohan and Seshadri (2004) used elastic plastic material model with plastic modulus of  $50 \times 10^4$  psi.

Evaluation of a remaining strength factor in the present study assumes a material model almost equivalent to elastic perfectly plastic behavior as shown in Fig 5.1. The Bilinear Kinematic Hardening (BKIN) option in ANSYS, which assumes that the structural materials possess a significant amount of reserve strength beyond their yield limit. Therefore, it is reasonable that a certain portion of the reserve strength could be taken into account while performing the assessment, given that the difference between the yield and ultimate strength of the material is considerably large. By taking the elastic-plastic material model and performing strain-based assessment, a portion of the reserve strength is taken into account, which reduces the conservatism and hence avoids the early repair or replacement of the component.

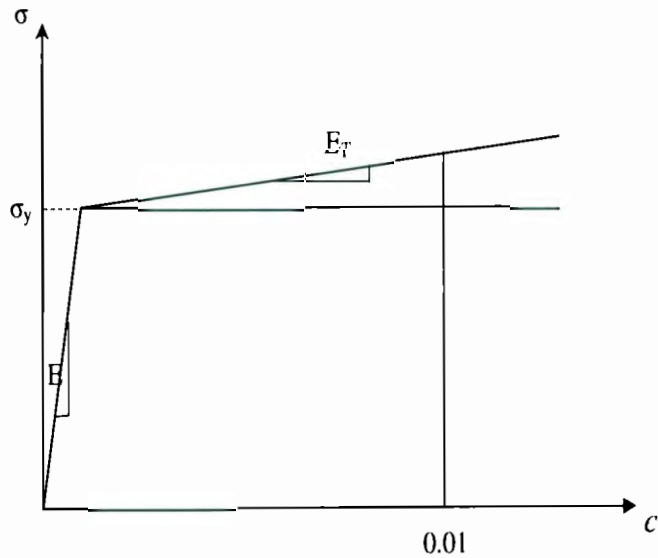


Figure 5.1 Material Model for Finite Element Analysis

Sims et al. [12] proposed a conservative limit on the amount of plastic strain in LTA based on numerous inelastic FEA. They argued that a limit of 2% plastic strain at any location provides a reasonable and conservative estimate of the actual collapse load of the structure. API 579 [1] recommends limiting the peak strain at any location of the remaining ligament to 5% when a Level 3 analysis is performed. In present analysis, 1 % plastic strain is considered as the limit for plastic collapse load estimation.

## 5.4 ILLUSTRATIVE EXAMPLE

In this section of the thesis, the estimation of the limit load and remaining strength factor of corroded storage tank with various configurations of corrosion profile is carried out. A liquid storage tank subjected to hydrostatic pressure, with no gas blanket pressure, is considered in this example in order to demonstrate the proposed Level 2 FFS assessment methods. The tank details are given below where the values given in the brackets are in SI units.

Shell inside radius ( $R_i$ )	:	512.0000 in. (13.0048 m)
Shell overall height (H)	:	394.0000 in. (10.0076 m)
Density of water (20°C) ( $\rho$ )	:	0.0369 lb/in <sup>3</sup> (998 kg/m <sup>3</sup> )
Operating pressure $p_o$	:	14.2282 psi (98.0999 kPa)
Design pressure $p_d$	:	16 psi (110.3160 kPa)
Allowable stress ( $S$ )	:	16,000 psi (110.3160 MPa)
Yield stress ( $\sigma_y$ )	:	30,000 psi (206.8430 MPa)
Corrosion allowance (CA)	:	1/16 in. = 0.0625 in (0.0016 m)
Joint efficiency	:	1.0

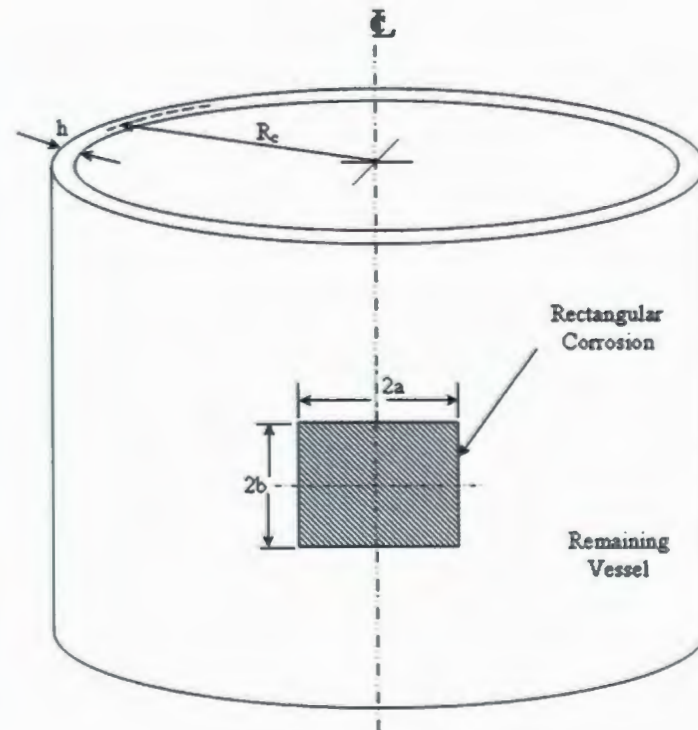


Figure 5.2 A schematic diagram of rectangular LTA in a storage tank

#### 5.4.1 Required Thickness calculation

For design conditions:

Design Thickness [25]:

$$t_d = \frac{(P_d \cdot R_i)}{S \cdot E - 0.6P_d}$$

$$= 0.5130 \text{ in. (0.0130 m)}$$

$$\text{Shell Thickness: } h = (t_d + \text{CA}) = 0.5755 \text{ in. (0.0146 m)}$$

Therefore 5/8 inch (0.0158 m) plate is considered.

#### 5.4.2 Calculation of Decay Lengths

Longitudinal ( $x_l$ ) and circumferential ( $x_c$ ) decay lengths are evaluated using Eq. (4.13) and Eq. (4.14), respectively as

$$x_l = 2.5\sqrt{Rh} = 44.7486 \text{ in. (1.1370 m)}$$

$$x_c = 6.3\sqrt{Rh} = 112.7665 \text{ in. (2.8630 m)}$$

#### Dimension of LTA:

For this calculation the area is considered as rectangular strip, circumferential and longitudinal dimensions of the LTA (Fig. 5.3) are considered as

$$2a = 100 \text{ in. (2.5400 m)};$$

$$2b = 100 \text{ in. (2.5400 m).}$$

The aspect ratio of the damaged area:  $(b/a) = 1.0$ .

$$\text{Shell outside radius (R)} = 512.6250 \text{ in. (13.0206 m)}$$

$$\text{Shell thickness (h)} = 0.625 \text{ in. (0.0159 m)}$$

$$\text{Corroded thickness (h}_c) = 0.1562 \text{ in. (0.0039 m)}$$

$$\text{Corroded radius (R}_c) = 512.1562 \text{ in. (13.0087 m)}$$

**Calculation of Reference Volume:** The reference volume is calculated as follows:

$$\text{Volume of LTA: } V_D = (4ab)h_c = 1,562.5001 \text{ in.}^3 \text{ (0.0256 m}^3\text{)}$$

Uncorroded Volume:

$$V_U = [(2x_c + 2a)(2x_l + 2b) - 4ab] h = 32,289.5600 \text{ in.}^3 \text{ (0.5291 m}^3\text{)}$$

Reference Volume:

$$V_R = (V_U + V_D) = 33,852.0601 \text{ in.}^3 \text{ (0.5550 m}^3\text{)}$$

### 5.4.3 Evaluation of Hydrostatic Equivalent Pressure and Corresponding Stresses

In order to apply the concept of decay lengths and reference volume, originally derived for pressure vessels and piping subjected to uniform internal pressure, equivalent hydrostatic pressure needs to be calculated for the kinematically active volume.

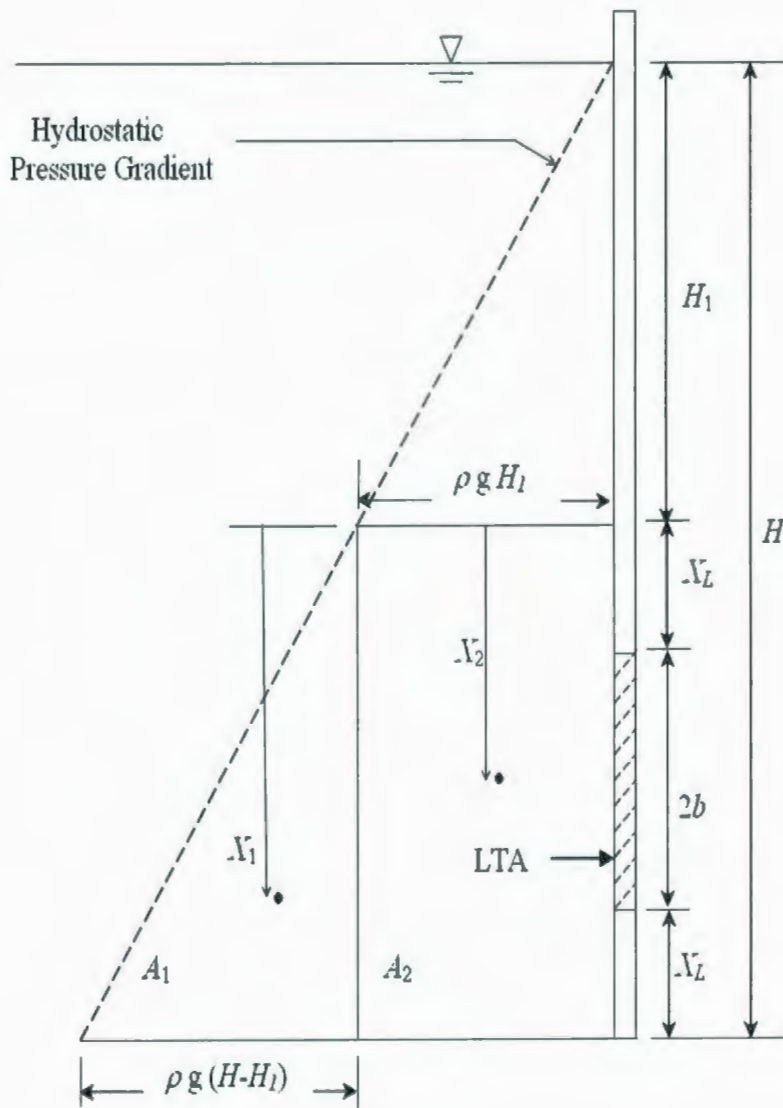


Figure 5.3 Evaluation of Hydrostatic Equivalent Pressure

$H_1 = \{H - (2x_1 + 2b)\}$  where  $H$  is the total height of the tank.

$H_1 = \{394 - (2 \times 44.74 + 100)\} = 204.5058 \text{ in. (5.1944 m)}$

For triangular area vertical distance from the fluid surface to the centroid of the area:

$$X_1 = \left\{ \left( \frac{2}{3} \right) \cdot (2X_L + 2b) + H_1 \right\}$$

$$= 330.8342 \text{ in (8.4031 m)}$$

For rectangular area vertical distance from the fluid surface to the centroid of the area:

$$X_2 = \left\{ \left( \frac{1}{2} \right) \cdot (2X_L + 2b) + H_1 \right\}$$

$$= 299.2514 \text{ in (5.1934 m)}$$

$$\text{Triangular Area of LTA } A_1 = \left[ \left( \frac{1}{2} \right) \{ \gamma (H - H_1) \} (2X_L + 2b) \right]$$

$$= 651.0201 \text{ lbf/in (113,073.1512 N/m)}$$

$$\text{Rectangular Area of LTA } A_2 = [(\gamma H_1) (2X_L + 2b)]$$

$$= 1,406.1701 \text{ lbf/in (244,040.0810 N/m)}$$

$$\text{Equivalent distance } \bar{X}_G = \frac{(A_1 x_1 + A_2 x_2)}{A_1 + A_2}$$

$$= 309.2140 \text{ in. (7.8540 m)}$$

Hydrostatic equivalent pressure on LTA:

$$p_{avg} = \bar{X}_G \rho g$$

$$= 11.1528 \text{ psi (76.8930 kPa)}$$

**Stresses in corroded region (LTA):**

$$\begin{aligned}\text{Hoop stress: } \sigma_{tc} &= \frac{p_{avg} R_c}{t_c} \\ &= 12.2150 \text{ ksi (84.2210 MPa)}\end{aligned}$$

**Stresses in uncorroded region:**

$$\begin{aligned}\text{Hoop Stress: } \sigma_t &= \frac{p_{avg} R}{t} \\ &= 9.1590 \text{ ksi (63.1470 MPa)}\end{aligned}$$

For this current work, hoop stress is considered here since the tank is subjected to differential hydrostatic pressure, without any blanket pressure.

Therefore,  $\sigma_{eu} = \sigma_t = 9.1590 \text{ ksi (63.1450 MPa)}$

$$\sigma_{ec} = \sigma_{tc} = 12.2150 \text{ ksi (84.2210 MPa)}$$

**5.4.4 Evaluation of Multipliers**

Upper bound multiplier for the undamaged tank:  $m_U^0 = \frac{\sigma_y}{\sigma_{eu}} = 3.2754$

Lower bound multiplier for the damaged tank:  $m_{Ld} = \frac{\sigma_y}{\sigma_{ec}} = 2.4552$

$$\text{Upper bound multiplier for damaged tank: } m_d^0 = \sqrt{\frac{\sigma_y^2 V_R}{\sigma_{eU}^2 V_U + \sigma_{eD}^2 V_D}} = 3.1710$$

The  $m_\alpha$ -tangent multiplier for damaged tank using Eq. (3.10):

$$m_\alpha^T = \frac{m^0}{1 + 0.2929(\zeta - 1)} = 2.9100;$$

$$\text{where } \zeta = \frac{m_d^0}{m_{Ld}}$$

## 5.5 RSF USING ANALYTICAL APPROACH

Three different RSFs are evaluated here using the aforementioned limit load multipliers.

$$\text{Using Eq. (3.26), } RSF_U = \frac{m_d^0}{m_u^0} = 0.970$$

$$\text{Using Eq. (3.27), } RSF^T = \frac{m_\alpha^T}{m_u^0} = 0.889$$

$$\text{Using Eq. (3.28), } RSF_L = \frac{m_{Ld}}{m_u^0} = 0.749$$

It should be noted that the above mentioned strength parameters (RSF) are evaluated using analytical expressions, and no FEA is required. A number of LTAs are considered further with different aspect ratios and corrosion depth. The results are given in Table 1 and Table 2.

## 5.6 RSF USING TWO LINEAR ELASTIC FEA

An alternative method for evaluating RSF based on the  $m_\alpha$ -tangent method is proposed here, which is evaluated using linear elastic FEA, circumventing need for decay lengths and reference volume, as is necessary in the analytical approach. In this case, the  $m_\alpha$ -tangent multiplier ( $m_\alpha^T$ ) is evaluated from the statically admissible stress field obtained from a linear elastic FEA. The structure is subjected to hydrostatic internal pressure without any blanket pressure.

From the initial linear elastic FEA of the corroded tank,  $m_f=1.991$  and  $m^0=4.391$  is evaluated using Eq. (3.5) and Eq. (3.9) respectively. The corresponding  $\zeta=2.205$  is calculated using Eq. (3.11). Then the value of the limit load multiplier is evaluated using Eq. (3.10) as  $m_\alpha^T=3.240$ . The same procedure is used to evaluate the limit load multiplier for uncorroded tank, which gives  $m_\alpha^T=3.650$ . Finally,  $RSF^T$ , based on linear elastic FEA, is evaluated as:

$$RSF^T = (m_\alpha^T|_{Corroded}) / (m_\alpha^T|_{Uncorroded}) = 0.887$$

## 5.7 RSF BASED ON INELASTIC FEA

Level 3 inelastic RSF is evaluated in order to verify the accuracy of Level 2 RSFs obtained from the proposed analytical and linear elastic FEA based methods. The same FE model as described in the previous section is used with plastic modulus of  $50 \times 10^4$  psi in order to account for the strain hardening effect. The inelastic RSF is calculated from the ratio of the limit pressure at 1% membrane strain in the LTA to the limit pressure of the tank without LTA. For this example,  $RSF_{inelastic}$  is evaluated as 0.916. The same procedure is applied to LTAs with different aspect ratios and corrosion depth. The results are tabulated in Table 5.1 and Table 5.2

Table 5-1

$a(\text{in.})$	$b(\text{in.})$	$r = b/a$	Analytical			LEFEA	NFEA
			$RSF_U$	$RSF_L$	$RSF_{m'_a}$	$RSF_{m'_a}$	$RSF_{inelastic}$
50.0	12.5	0.25	0.9932	0.7490	0.9120	0.9101	0.9930
50.0	25.0	0.50	0.9800	0.7490	0.9050	0.8910	0.9250
50.0	50.0	1.00	0.9701	0.7490	0.8891	0.8877	0.9160
50.0	75.0	1.50	0.9769	0.7490	0.8900	0.8890	0.9090
50.0	100.0	2.00	0.9650	0.7490	0.8900	0.8700	0.8961

Table 5.1 RSF for Liquid Storage Tank having LTA with 25% corrosion

Table 5-2

$a(in.)$	$b(in.)$	$r = b/a$	Analytical			LEFEA	NFEA
			$RSF_U$	$RSF_L$	$RSF_{m_a^T}$	$RSF_{m_a^T}$	$RSF_{inelastic}$
50.0	12.5	0.25	0.9520	0.4900	0.7803	0.8040	0.8800
50.0	25.0	0.50	0.9291	0.4900	0.7430	0.7473	0.7631
50.0	50.0	1.00	0.8903	0.4900	0.7300	0.7401	0.7990
50.0	75.0	1.50	0.8701	0.4900	0.7151	0.7360	0.7492
50.0	100.0	2.00	0.8584	0.4900	0.7104	0.7200	0.7301

Table 5.2 RSF for Liquid Storage Tank having LTA with 50% corrosion

## 5.8 DISCUSSION

Level 2 Fitness-for-Service assessment methods are developed in this current research to estimate the remaining strength factor of liquid storage tank experiencing hydrostatic pressure having locally thinned areas. The procedure is based on variational principles of plasticity, used in conjunction with the reference volume approach, has been found to be a very simple and straight forward method for integrity assessment purposes.

The Level 2 integrity assessment procedures is applied to rectangular locally thinned areas (LTA) and sample calculations for evaluating RSF is presented. Two different approaches are proposed in the present work to evaluate RSF. The first approach is based on an analytical method and the second approach is based on linear elastic finite element analysis (LEFEA). Both methods are applied to LTA for a range of sizes and corroded thickness, and results are compared with inelastic finite element analysis results. The RSF2 that based on  $m_\alpha$ -tangent multiplier ( $m_\alpha^T$ ) found to be conservative, and comparable with the inelastic FEA. Therefore, the use of RSF2 is recommended for Fitness-for-Service evaluations.

The proposed assessment method is a simple step-by-step procedure that should be attractive to plant engineers and designers. Remaining Strength Factor (RSF) can be evaluated using proposed analytical expressions, and no FEA is required. The second method RSF can also be evaluated using two linear elastic finite analysis, avoiding the identification of decay lengths and reference volume as is necessary in analytical approach. The results obtained using these two approaches are in good agreement with each other.

## CHAPTER 6

### CONCLUSIONS, RECOMMENDATIONS AND FUTURE WORK

#### 6.1 CONTRIBUTIONS OF THE THESIS

In this thesis two different approaches are proposed to evaluate Remaining Strength Factor (RSF) for liquid storage tanks containing corrosion damage. The first method is a simple analytical approach, and the second method is based on two linear elastic finite element analyses (LEFEA). The methods are based on variational concepts,  $m_\alpha$ -tangent multipliers, reference volume and the concept of decay lengths in cylindrical shells.

The principles leading to an improved lower bound limit load called the  $m_\alpha$ -tangent method (as developed in earlier studies) are discussed in detail in chapter 3. The  $m_\alpha$ -tangent method has been shown to provide acceptable approximations to limit load of various mechanical components, and thus is employed as the basis of the calculation of the recommended remaining strength factors proposed in the current study.

The concept of reference volume is used in this current thesis which gives better approximation of limit load multipliers than using the entire volume of the structure. The effects of local loads on a shell structure are normally restricted to a limited volume in the vicinity of the loads. This kinematically active volume participates in plastic action when local damage occurs in a component and is termed as the reference volume. This reference volume approach gives better estimation of remaining strength factor.

Both the methods are demonstrated through examples. Inelastic finite element analysis also has been carried out in this current research in order to compare the results obtained by the proposed methods. Strain hardening was accounted in this present work to take advantage of the post-yield behavior of high strength steels in inelastic finite element analysis.

## **6.2 Future Effort**

In this thesis, Level 2 FFS assessment methods are proposed for estimating the strength parameter for liquid storage tanks containing “locally thin areas”. In this current research, an irregular profile of corrosion damage is represented by an equivalent rectangular damaged area in cylindrical storage tank. Corrosion spots observed in storage tanks in-service are usually irregular.

Although the proposed approach assumes uniform damage and does not account for the irregularity, the methods can be extended to determine the remaining strength factors for an irregular profile including irregular damaged area and thickness loss. The level 2 Assessment rules of API 579 (Sec. 5.4.1.2) provide for an estimate of the structural integrity of a component when significant variations in the thickness profile occur within the region of metal loss.

Current API 579 rules for FFS assessment covers LTA remote from major structural discontinuities. Also in this current research two adjacent damage areas are also assumed not to interact. The interaction of LTAs is one of the problems encountered in the industry. Procedures to calculate the remaining strength factor of pressure vessels with damaged spots near structural discontinuities and multiple interacting damaged spots need to be studied.

The proposed Fitness-for-Service assessments in the current research have been shown to offer lower bound remaining strength factor estimates to pressure vessels of cylindrical shapes. The proposed methods should be extended for spherical liquid storage tanks experiencing hydrostatic pressure.

Another potential area of research is the extension of this method for liquid storage tanks having different shell thickness and locally thin areas in between two shell thickness. An experimental study with strain gauges set up can be conducted to obtain the collapse pressure of a corroded component as well as to investigate the behavior of the damaged pressure components at limit state. Results from such experiments can be used to validate the accuracy and effectiveness of the proposed methods.

### 6.3 CONCLUSIONS

Level 2 FFS assessment methods are proposed in this research to estimate the strength parameter for evaluating industrial storage tanks containing locally thin areas. The integral mean of yield criterion in conjunction with the  $m_\alpha$ -tangent method is used to develop the proposed Level 2 RSF. The RSF obtained by using the  $m_\alpha$ -tangent method is shown to be conservative and is in good agreement with the inelastic analysis based Level 3 RSF. Using the proposed method, reasonably accurate RSF estimates can be obtained on the basis of two linear elastic FEA or analytically. The  $RSF^T$  based on the  $m_\alpha$ -tangent method is suggested as a parameter for performing FFS assessment of liquid storage tanks undergoing corrosion damage.

## PUBLICATIONS

- **F.Ahmad**, M.M.Hossain, R.Seshadri, "Fitness-for-Service Assessment of Hydrocarbon Storage Tanks," ASME Journal of Pressure Vessel Technology, 2009 Accepted.
- "Summary and Comparison of Fitness-for-Service Assessment of Hydrocarbon Storage Tanks," presented at the Aldrich Conference 2009 in St. John's, NL

## REFERENCES

- [1] API, 2000, "Recommended Practice for Fitness-for-Service," API 579, American Petroleum Institute, Washington DC.
- [2] R6, 2001, "Assessment of Integrity of Structures Containing Defects," Revision 4, British Energy.
- [3] SINTAP, 1999, "Structural Integrity Assessment Procedure for European Industry," Project BE95-1426. Final Procedure, British Steel Report, Brussels: Brite Euram Programme.
- [4] Kniefner JF, Vieth P.H, 1989, "A Modified Criterion for Evaluating the Remaining Strength of Corroded Pipe (with RSTRENG)," American Gas Association, Catalogue L51609, PR3-805.
- [5] Seshadri, R., 2005. "Integrity Assessment of Pressure Components with Local Hot Spots". ASME J. Pressure Vessel Technol., 127, pp. 137-142.
- [6] Seshadri, R., and Mangalaramanan, S. P., 1997, "Lower Bound Limit Loads Using Variational Concepts: the  $m_n$ -method," Int. J. Pressure Vessels & Piping, 71, pp. 93-106.
- [7] Indermohan, H. and Seshadri, R., 2005. "Fitness-for-service Methodology based on Variational Principles in Plasticity". ASME J. Pressure Vessel Technol., 127, pp. 92-97.

- [8] Ramkumar, B. and Seshadri R., June 2005. "Fitness for Service Assessment of Corroded Pipelines based on Variational Principles in Plasticity". *Journal of Pipeline Integrity*, 2, pp. 99-116.
- [9] ASME, 1984. *Manual for Determining the Remaining Strength of Corroded Pipelines*, American National Standards Institute (ANSI)/ American Society of Mechanical Engineers (ASME) B31G.
- [10] Tantichattanont, P., Adluri, S., and Seshadri, R., 2006, "Structural Integrity Evaluation for Corrosion in Spherical Pressure Vessels" *Int. J. Pressure Vessels & Piping*, 84, pp. 749-761.
- [11] Reinhardt W. D., and Seshadri R., 2003, "Limit Load Bounds for the  $m_a$ -Multipliers," *ASME J. Pressure Vessel Technol.*, 125, pp.11- 18.
- [12] Sims, J. R., Hantz, B. F., Kuehn, K. E., "A Basis for the Fitness for Service Evaluation of Thin Areas in Pressure Vessels and Storage Tanks" *Pressure Vessel Fracture, Fatigue, and Life management*, ASME PVP 1992, 233, pp. 51-8.
- [13] Seshadri, R. and Hossain, M. M., 2008, "Simplified Limit Load Determination Using the  $m_a$ -Tangent Method", *ASME Pressure Vessels and Piping Division Conference*, Paper No. PVP2008-61171, July 27-31, Chicago, Illinois, USA.
- [14] Tantichattanont, P., Adluri, S. M. R., and Seshadri, R., 2007, "Fitness-for-Service Evaluation of Thermal Hot Spots and Corrosion Damage in Cylindrical Pressure

Components,” ASME PVP, Paper No. PVP2007-26704, San Antonio, Texas, USA.

- [15] ANSYS, 2008, University Research Version 11.0, SASIP Inc.
  
- [16] Munson R., Young F., Okiishi H., Fundamentals of Fluid Mechanics, John Wiley & Sons, New York, USA.
  
- [17] Pattaramon Tantichattanon “Fitness-for-Service Assessment for Thermal Hot Spots and Corrosion in Pressure Vessels”, PhD Thesis.
  
- [18] API, 1994, “Welded Steel Tanks for Oil Storage,” API 650, American Petroleum Institute, Washington DC.
  
- [19] Reinhardt, W. D., and Seshadri, R., 2003, “Limit Load Bounds for the  $m_r$ -Multiplier,” ASME J. Pressure Vessel Technol., 125, pp. 11-18.
  
- [20] API, 1996, “Design and Construction of Large, Welded, Low-Pressure Storage Tanks” API 620, American Petroleum Institute, Washington DC.
  
- [21] 2007, ASME Boiler and Pressure Vessel Code, Section III, New York.
  
- [22] 2007, ASME Boiler and Pressure Vessel Code, Section VIII, Division 2, New York.
  
- [23] Adibi-Asl, R., and Seshadri, R., 2007, “Simplified Limit Load Determination Using the Reference Two-Bar Structure ,” ASME Paper No. PVP 2007-26747

- [24] Arthur P.Boresi., Richard J.Schmidt, 1993. *Advanced Mechanics of Materials*, Fifth Edition. John Wiley & Sons, Inc.,New York.
- [25] Bednar, H. H., 1985. *Pressure Vessel Design Handbook*. Second Edition, Van Nostrand Reinhold Company, New York.
- [26] Beer, F. P., Johnston, E. R., Jr. and DeWolf, J. T., 2002. *Mechanics of Materials*, Third Edition. McGraw-Hill Companies, Inc.
- [27] Bolar, A. A. and Adluri, S. M. R., 2005. "Robust Estimation of Limit Loads of Plates." *33rd Annual General Conference of the Canadian Society of Civil Engineering*, Toronto, ON, Canada. June 2-4, 2005.
- [28] Calladine, C. R., 1983. *Theory of Shell Structures*. Cambridge University Press, Cambridge.
- [29] Calladine, C. R., 2000. *Plasticity for Engineers: Theory and Application*. Horwood Publishing, Chichester.
- [30] Myers, P.E, 1997. *Aboveground Storage Tanks*, McGraw-Hill Companies, Inc.
- [31] [www.icheme.org](http://www.icheme.org) Bp Process Safety Series: Safe Tank Farms and (Un) loading Operations.
- [32] Antaki, G, 2005. *Fitness-for-Service and Integrity of Piping, Vessels, and Tanks*. ASME CODE SIMPLIFIED, McGraw-Hill Companies, Inc.

- [33] Brian, D. 2004. *The Above Ground Steel Storage Tank Handbook*, John Wiley & Sons, Inc., New York.
- [34] Alex, M. 1983. *Petroleum Storage Principles*, PennWell Books, Oklahoma.
- [35] J.D. Harston, 2007. *Corrosion in Refineries*, CRC Press, New York.
- [36] Jones, R. D., 1991. *Stress Analysis of High Temperature Storage tanks*. Master's Thesis, University of Regina, Regina, Saskatchewan, Canada.
- [37] Smith, J. H., Rana, M. D. and Hall, C., 2003. "The Use of "Fitness for Service" Assessment Procedures to Establish Critical Flaw Sizes in High-Pressure Gas Cylinders." *Journal of Pressure Vessel Technology, Transactions of the ASME*, **125(2)**, pp. 177-181.
- [38] Janosch, J. J., Huther, M., Kocak, M. and Taylor, N., 2005. "European Fitness-for-Service Network (FITNET) – Fatigue Module Development." *Proceedings of the International Conference on Offshore Mechanics and Arctic Engineering – OMAE*, **3**, pp.329-338.
- [39] Jaske, C. E. and Beavers, J. 2000. "Fitness-for-service Assessment for Pipelines Subject to Stress-Corrosion Cracking." *Corrosion Prevention and Control*, **47(1)**, pp. 15-24. Jones, D. G., Turner, T. and Ritchie, D., 1992. "Failure Behavior of Internally Corroded Linepipe." *British Gas plc*, OMAE-92-1045.

- [40] Kocak, M., 2005. "Fitness for Service Analysis of Structures Using the FITNET Procedure: An Overview." *Proceedings of the International Conference on Offshore Mechanics and Arctic Engineering – OMAE*, **3**, pp. 321-328.
- [41] Kuvin, B. F., 1991. "Fitness for Service-Steady Progress." *Welding Design & Fabrication*. **64**, pp. 32.
- [42] McCabe, J. F., 2002. "Fitness for service evaluations and non-linear analysis – 2000." *ASME Pressure Vessels and Piping Division (Publication) PVP*, **442**, 173p.
- Milne, I., Ainsworth, R. A., Dowling, A. R., and Stewart, A. T., 1988. "Assessment of the Integrity of Structures Containing Defects." *International Journal of Pressure Vessels and Piping*, **32**, pp. 3-104
- [43] Osage, D. A., Janelle, J., and Henry, P. A., 2000. "Fitness-For-Service Local Metal Loss Assessment Rules in API 579", *ASME Pressure Vessels Piping Div Publ PVP*, **411**, pp. 143-176
- [44] Pan, L., 2003. *Limit Load Estimation for Structures Under Mechanical Loads*. Ph. D. Dissertation. Faculty of Engineering and Applied Science, Memorial University of Newfoundland, St. John's
- [45] Rodery, C. D., Takagi, Y., Mura, N. Seipp, T. G., Iyer, S., Cohn, M. J. and McCabe, J.F., 2004. "Fitness for Service, Life Extension, Remediation, Repair, and

Erosion/Corrosion Issues for Pressure Vessels and Components – 2004. *ASME Pressure Vessels and Piping Division PVP*, **471**, 171 p.

- [46] Sehgal, R., Tiwari, A. and Sood, V., 2005. "A Study on Fitness-for-service Assessment for Crack-like Defects and Corrosion in Nuclear Reactor Pressure Tubes." *Reliability Engineering and System Safety*, **89(2)**, pp. 227-235.
  
- [47] Osage, D. A., 1997. "New Development in API 579." *International Journal of Pressure Vessels and Piping*, **71**, pp. 93-106.
  
- [48] Osage, D. A., Krishnaswamy, P. , Stephens, D.R., Scott, P., Janelle, J., Mohan, R., Wilkowski, G. M., 2001. "Technologies for the evaluation of non-crack-like flaws in pressurized components-erosion/corrosion, pitting, blisters, shell out-of-roundness, weld misalignment, bulges and dents." *Welding Research Council Bulletin*, **465**, pp. 1-25.
  
- [49] Harvey, J. F., 1991. *Theory and Design of Pressure Vessels*, Second Edition. Chapman & Hall, New York.
  
- [50] Kraus, H., 1967. *Thin Elastic Shell*. John Wiley & Son, Inc., New York.
  
- [51] Mendelson, A., 1968. *Plasticity: Theory and Application*. MacMillan Company, New York.
  
- [52] ASME Boiler and Pressure Vessel Code, 2007, Section III, American Society of Mechanical Engineers, New York, USA.

## Appendix A

ANSYS batch files are used to perform the finite element analysis of storage tanks containing corrosion damage as discussed in Chapter 5 are provided in this section. The analysis type includes both elastic and inelastic finite element analysis.

### A.1 Linear Analysis of Storage Tank without Corrosion Subjected to Internal Pressure

```
/Title Linear Analysis of Storage Tank under Internal Pressure
```

```
/config, nproc/4
```

```
/prep7
```

```
!Material Properties
```

```
ET,1,SOLID185
```

```
MP,EX,1,30e6
```

```
! Modulus of Elasticity
```

```
MP,PRXY,1,0.3
```

```
! Poisson's Ratio
```

```
Ri=512
```

```
t=0.625
```

```
Ro=512.625
```

```
Len=394
```

! Solid modeling

K, 1,0,0,0

K, 2, Ro, 0, 0

K, 3, Ri, 0, 0

K, 4, 0, 0,-Ro

K, 5, 0, 0,-Ri

K, 6, 0, Len, 0

LARC, 2, 4, 1, Ro

LARC, 3, 5, 1, Ri

L, 2,3

L, 4,5

L, 1,6

al,1,3,2,4

VDRAG,1,,,,,5

! Mapped Meshing

lesize,12,,,150

! Across Length

lesize,7,,,150

! Across Length

lesize,11,,,280

! Circumferentially

lesize,6,,,280

! Circumferentially

lesize,13,,,4

lesize,3,,,4

vmesh,All

!Apply Boundary Conditions

DA,5,SYMM

DA,3,SYMM

DA,1,UX,0

DA,1,UY,0

DA,1,UZ,0

! Load Application

SFGRAD,PRES,0,Y,0,-0.04061

NSEL,all

SFA,4,1,PRES,16,0

DTRAN

SFTRAN

finish

/SOLU

ANTYPE,0

solve

save

finish

## A.2 Non-linear Analysis of Storage Tank without Corrosion Subjected to Internal Pressure

/ Title Non-linear Analysis of Storage Tank under Internal Pressure

/ config,nproc/4

/ prep7

IMMED,1

! MAterial Properties

ET,1,SOLID185

MP,EX,1,30e6

MP,PRXY,1,0.3

TB,BKIN,1,1,2,1 ! Bilinear kinematic strain hardening

TBDATA,,30000,0 ! Data table, yield stress, plastic modulus

Ri=512

t=0.625

Ro=512.625

Len=394

! Solid modeling

K,1,0,0,0

k,2,Ro,0,0

```
k,3,Ri,0,0
k,4,0,0,-Ro
k,5,0,0,-Ri
K,6,0,Len,0
LARC,2,4,1,Ro
LARC,3,5,1,Ri
L,2,3
L,4,5
L,1,6
al,1,3,2,4
VDRAG,1,,,,,5
!Mapped Meshing

lesize,12,,,150 ! Across Length
lesize,7,,,150 ! Across Length
lesize,11,,,280 ! Circumferentially
lesize,6,,,280 ! Circumferentially
lesize,13,,,4
lesize,3,,,4
vmesh,All

!Apply Boundary Conditions

DA,5,SYMM
```

DA,3,SYMM

DA,1,UX,0

DA,1,UY,0

DA,1,UZ,0

!Load Application

SFGRAD,PRES,0,Y,0,-0.81218274

NSEL,all

SFA,4,1,PRES,320,0

DTRAN

SFTRAN

finish

/SOLU

ANTYPE,0

NSUBST,2000 ! Initial number of substep

/output,out,dat

solve

save

finish

### **A.3 Linear Analysis of Storage Tank with Corrosion Depth 25% Subjected to Internal Pressure**

/Title, Linear Analysis of Storage Tank with Corrosion Depth 25%

/prep7

IMMED,1

!SOLID MODELLING Storage Tank

!MAterial Properties

ET,1,SOLID185

MP,EX,1,30e6

MP,PRXY,1,0.3

Ro=512.625

t=0.625

Ri=512

theta=5.59

b=100

xl=44.748

xb=144.748

Len=394

\*set,dc,0.15625

\*set,Rc,512.15625

```

*set,P,16

! Calculation of ARC Length

pi=3.141592654
arc1=(1.57*Rc)
arc4=(1.57* Ri)
arc5=(1.57*Ro)
arc2=(pi*theta*Rc)/180
arc3=(pi*theta*Ri)/180
arc6=(pi*theta*Ro)/180

a=arc2/arc1
a1=arc3/arc4
a2=arc6/arc5

! Element Size

Lon_Upper =95      ! No of elements along axial Direction above 2b
x1_DIV =17        ! No of elements along axial direction below 2b
b_DIV=38          ! No of elements along longitudinal direction in 2b
theta_div=20      ! No of elements along Circumferential Direction in the LTA
ARC_DIV1=260     ! No of elements along Circumferential direction in

Undamaged region

tc_Div=3          ! Number of elements along corrosion depth
t_div=1          ! Number of elements along remaining thickness of the pipe

!Solid modelling

K,1,0,0,0

```

k,2,Ro,0,0

k,3,Ri,0,0

k,4,0,0,-Ro

k,5,0,0,-Ri

K,6,0,Len,0

! New location for Corrosion

K,7,0,xl,0

K,8,Ro,xl,0

K,9,Ri,xl,0

K,10,0,xl,-Ro

K,11,0,xl,-Ri

LARC,3,5,1,Ri

LARC,2,4,1,Ro

LARC,9,11,7,Ri

LARC,8,10,7,Ro

L,3,2

L,5,4

L,1,6

L,1,7

L,8,9

L,10,11

al,1,2,5,6

VDRAG,1,,,,,7

! Corrosion Construction

k,20,0,xl,-Rc

k,21,Rc,xl,0

LARC,20,21,7,Rc

LDIV,19,a,71

LDIV,3,1-a,81

L,71,81

LCSL,19,10

al,24,19,22,21

vext,7,,,b

vsbv,1,2

! Modification of Volume for Mapped Meshing

LDIV,4,1-a2,101

L,71,101

LDIV,11,1-a2,102

LDIV,16,a1,103

L,102,103

LDIV,1,1-a2,302

LDIV,2,1-a1,301

L,302,301

a,103,301,302,102

VSBA,3,2

k,54,(Ro+10),xl,-(Ro+10)

k,55,-(Ro+10),xl,-(Ro+10)

k,56,-(Ro+10),xl,(Ro+10)

k,57,(Ro+10),xl,(Ro+10)

A,54,55,56,57

VSBA,1,1

k,54,(Ro+10),xl,-(Ro+10)

k,55,-(Ro+10),xl,-(Ro+10)

k,56,-(Ro+10),xl,(Ro+10)

k,57,(Ro+10),xl,(Ro+10)

A,54,55,56,57

VSBA,2,1

k,54,(Ro+10),xb,-(Ro+10)

k,55,-(Ro+10),xb,-(Ro+10)

k,56,-(Ro+10),xb,(Ro+10)

k,57,(Ro+10),xb,(Ro+10)

A,54,55,56,57

VSBA,4,1

k,54,(Ro+10),xb,-(Ro+10)

k,55,-(Ro+10),xb,-(Ro+10)

k,56,-(Ro+10),xb,(Ro+10)

k,57,(Ro+10),xb,(Ro+10)

A,54,55,56,57

VSBA,5,1

! Finite Element Mode and Meshing

! Set the Element Division

lesize,67,,,Lon\_Upper

lesize,33,,,Lon\_Upper

lesize,42,,,Lon\_Upper

lesize,62,,,Lon\_Upper

lesize,41,,,Lon\_Upper

lesize,59,,,Lon\_Upper

lesize,46,,,x1\_DIV

lesize,32,,,x1\_DIV

lesize,50,,,x1\_DIV

lesize,43,,,x1\_DIV

lesize,47,,,x1\_DIV

lesize,49,,,x1\_DIV

lesize,35,,,Arc\_Div1

lesize,11,,,Arc\_Div1

lesize,58,,,Arc\_Div1

lesize,61,,Arc\_Div1

lesize,20,,Arc\_Div1

lesize,3,,Arc\_Div1

lesize,48,,Arc\_Div1

lesize,4,,Arc\_Div1

lesize,51,,Arc\_Div1

lesize,1,,Arc\_Div1

lesize,2,,Arc\_Div1

lesize,16,,theta\_Div

! Rectangular Strip

lesize,34,,theta\_Div

lesize,55,,theta\_Div

lesize,25,,theta\_Div

lesize,27,,theta\_Div

lesize,21,,theta\_Div

lesize,19,,theta\_Div

lesize,45,,theta\_Div

lesize,13,,theta\_Div

lesize,37,,theta\_Div

lesize,38,,theta\_Div

lesize,28,,tc\_Div

lesize,53,,tc\_Div

lesize,23,,tc\_Div

lesize,44,,tc\_Div

lesize,63,,tc\_Div

lesize,54,,tc\_Div

lesize,26,,t\_Div

lesize,10,,t\_Div

lesize,24,,t\_Div

lesize,22,,t\_Div

lesize,29,,b\_Div

lesize,56,,b\_Di

lesize,31,,b\_Div

lesize,30,,b\_Div

lesize,64,,b\_Div

lesize,65,,b\_Div

lesize,66,,b\_Div

! Reverse line Directions to obtain the Desired Gradually varying Mesh

LREVERSE,33

LREVERSE,35

LREVERSE,41

LREVERSE,59

LREVERSE,3

LREVERSE,48

LREVERSE,4

LREVERSE,51

LREVERSE,1

LREVERSE,2

! Concatenate Lines and Areas to Enable Mapped Meshing

! Joint

LCCAT,26,63

LCCAT,10,54

LCCAT,23,24

LCCAT,44,24

LCCAT,22,28

LCCAT,22,53

! Circumferentially Corrosion-Without corrosion

LCCAT,55,61

! Longitudinally

LCCAT,56,67

LCCAT,56,46

LCCAT,64,62

LCCAT,64,50

LCCAT,31,42

LCCAT,31,43

ACCAT,7,5

ACCAT,8,23

ACCAT,31,11

VMESH,ALL

! Boundary Conditions

DA,19,SYMM

DA,34,SYMM

DA,6,SYMM

DA,15,SYMM

DA,24,SYMM

DA,35,SYMM

DA,17,UX,0

DA,17,UY,0

DA,17,UZ,0

DA,3,UX,0

DA,3,UY,0

DA,3,UZ,0

DTRAN ! Transfer Boundary Conditions From Solid to FE model

SFTRAN ! Transfer Loads From Solid to FE Model

! Load Application

SFGRAD,PRES,0,Y,0,-0.040609137

NSEL,all

SFA,20,1,PRES,16,0

SFA,2,1,PRES,16,0

SFA,10,1,PRES,16,0

SFA,32,1,PRES,16,0

SFA,21,1,PRES,16,0

SFA,14,1,PRES,16,0

DTRAN

SFTRAN

Finish

/SOLU

ANTYPE,0

solve

save

finish

#### A.4 Non-linear Analysis of Storage Tank with Corrosion Depth 25% Subjected to Internal Pressure

/Title, Nonlinear Analysis of Storage Tank with Corrosion Depth 25%

/config, nproc/4

/prep7

IMMED,1

!SOLID MODELLING Storage Tank

!MAterial Properties

ET,1,SOLID185

MP,EX,1,30e6

MP,PRXY,1,0.3

TB,BKIN,1,1,2,1

! Bilinear kinematic strain hardening

TBDATA,,30000,0

! Data table, yield stress, plastic

modulus

Ro=512.625

t=0.625

Ri=512

theta=5.59

b=100

:l=44.748

xb=144.748

Len=394

\*set,dc,0.15625

\*set,Rc,512.15625

\*set,P,16

! Calculation of ARC Length

pi=3.141592654

arc1=(1.57\*Rc)

arc4=(1.57\* $R_i$ )

arc5=(1.57\* $R_o$ )

arc2=(pi\*theta\*Rc)/180

arc3=(pi\*theta\* $R_i$ )/180

arc6=(pi\*theta\* $R_o$ )/180

a=arc2/arc1

a1=arc3/arc4

a2=arc6/arc5

! Element Size

Lon\_Upper =95

! No of elements along axial Direction above 2b

x1\_DIV =17

! No of elements along axial direction below 2b

b\_DIV=38

! No of elements along longitudinal direction in

2b

theta\_div=20

! No of elements along Direction in the LTA

ARC\_DIV1=260

! No of elements along Undamaged region

tc\_Div=3

! Number of elements along corrosion depth

```
t_div=1                                ! Number of elements of the pipe

!Solid modelling

K,1,0,0,0

k,2,Ro,0,0

k,3,Ri,0,0

k,4,0,0,-Ro

k,5,0,0,-Ri

K,6,0,Len,0

!New location for Corrosion

K,7,0,xl,0

K,8,Ro,xl,0

K,9,Ri,xl,0

K,10,0,xl,-Ro

K,11,0,xl,-Ri

LARC,3,5,1,Ri

LARC,2,4,1,Ro

LARC,9,11,7,Ri

LARC,8,10,7,Ro

L,3,2

L,5,4

L,1,6

L,1,7

L,8,9
```

L,10,11  
al,1,2,5,6  
VDRAG,1,,,,,7  
!Corrosion Construction  
k,20,0,xl,-Rc  
k,21,Rc,xl,0  
LARC,20,21,7,Rc  
LDIV,19,a,71  
LDIV,3,1-a,81  
L,71,81  
LCSL,19,10  
al,24,19,22,21  
vext,7,,,b  
vsbv,1,2  
! Modification of Volume for Mapped Meshing  
LDIV,4,1-a2,101  
!L,81,101 (Previous Command working)  
L,71,101  
LDIV,11,1-a2,102  
LDIV,16,a1,103  
L,102,103  
LDIV,1,1-a2,302  
LDIV,2,1-a1,301

L,302,301

a,103,301,302,102

VSBA,3,2

k,54,(Ro+10),xl,-(Ro+10)

k,55,-(Ro+10),xl,-(Ro+10)

k,56,-(Ro+10),xl,(Ro+10)

k,57,(Ro+10),xl,(Ro+10)

A,54,55,56,57

VSBA,1,1

k,54,(Ro+10),xl,-(Ro+10)

k,55,-(Ro+10),xl,-(Ro+10)

k,56,-(Ro+10),xl,(Ro+10)

k,57,(Ro+10),xl,(Ro+10)

A,54,55,56,57

VSBA,2,1

k,54,(Ro+10),xb,-(Ro+10)

k,55,-(Ro+10),xb,-(Ro+10)

k,56,-(Ro+10),xb,(Ro+10)

k,57,(Ro+10),xb,(Ro+10)

A,54,55,56,57

VSBA,4,1

k,54,(Ro+10),xb,-(Ro+10)

k,55,-(Ro+10),xb,-(Ro+10)

k,56,-(Ro+10),xb,(Ro+10)

k,57,(Ro+10),xb,(Ro+10)

A,54,55,56,57

VSBA,5,1

! Finite Element Model and Meshing

! Set the Element Division

lesize,67,,,Lon\_Upper

lesize,33,,,Lon\_Upper

lesize,42,,,Lon\_Upper

lesize,62,,,Lon\_Upper

lesize,41,,,Lon\_Upper

lesize,59,,,Lon\_Upper

lesize,46,,,xl\_DIV

lesize,32,,,xl\_DIV

lesize,50,,,xl\_DIV

lesize,43,,,xl\_DIV

lesize,47,,,xl\_DIV

lesize,49,,,xl\_DIV

lesize,35,,,Arc\_Div1

lesize,11,,,Arc\_Div1

lesize,58,,,Arc\_Div1

lesize,61,,,Arc\_Div1

lesize,20,,,Arc\_Div1

lesize,3,,,Arc\_Div1  
lesize,48,,,Arc\_Div1  
lesize,4,,,Arc\_Div1  
lesize,51,,,Arc\_Div1  
lesize,1,,,Arc\_Div1  
lesize,2,,,Arc\_Div1  
lesize,16,,,theta\_Div ! Rectangular Strip  
lesize,34,,,theta\_Div  
lesize,55,,,theta\_Div  
lesize,25,,,theta\_Div  
lesize,27,,,theta\_Div  
lesize,21,,,theta\_Div  
lesize,19,,,theta\_Div  
lesize,45,,,theta\_Div  
lesize,13,,,theta\_Div  
lesize,37,,,theta\_Div  
lesize,38,,,theta\_Div  
lesize,28,,,tc\_Div  
lesize,53,,,tc\_Div  
lesize,23,,,tc\_Div  
lesize,44,,,tc\_Div  
lesize,63,,,tc\_Div  
lesize,54,,,tc\_Div

lesize,26,,,t\_Div

lesize,10,,,t\_Div

lesize,24,,,t\_Div

lesize,22,,,t\_Div

lesize,29,,,b\_Div

lesize,56,,,b\_Div

lesize,31,,,b\_Div

lesize,30,,,b\_Div

lesize,64,,,b\_Div

lesize,65,,,b\_Div

lesize,66,,,b\_Div

! Reverse line Directions to obtain the Desired Grdually varying Mesh

LREVERSE,33

LREVERSE,35

LREVERSE,41

LREVERSE,59

LREVERSE,3

LREVERSE,48

LREVERSE,4

LREVERSE,51

LREVERSE,1

LREVERSE,2

! Concatenate Lines and Areas to Enable Mapped Meshing

! Joint

LCCAT,26,63

LCCAT,10,54

LCCAT,23,24

LCCAT,44,24

LCCAT,22,28

LCCAT,22,53

! Circumferentially Corrosion-Without Corrosion

LCCAT,55,61

!Longitudinally

LCCAT,56,67

LCCAT,56,46

LCCAT,64,62

LCCAT,64,50

LCCAT,31,42

LCCAT,31,43

ACCAT,7,5

ACCAT,8,23

ACCAT,31,11

VMESH,ALL

! Boundary Conditions

DA,19,SYMM

DA,34,SYMM

DA,6,SYMM

DA,15,SYMM

DA,24,SYMM

DA,35,SYMM

DA,17,UX,0

DA,17,UY,0

DA,17,UZ,0

DA,3,UX,0

DA,3,UY,0

DA,3,UZ,0

DTRAN

! Transfer Boundary From Solid to FE

model

SFTRAN

! Transfer Loads From Solid to FE Model

! Load Application

SFGRAD,PRES,0,Y,0,-0.81218274

NSEL,all

SFA,20,1,PRES,320,0

SFA,2,1,PRES,320,0

SFA,10,1,PRES,320,0

SFA,32,1,PRES,320,0

SFA,21,1,PRES,320,0

SFA,14,1,PRES,320,0

DTRAN

SFTRAN

finish

/SOLU

ANTYPE,0

NSUBST,2000

! Initial number of substep

/output,out,dat

solve

save

finish







